

Using volcaniclastic rocks to constrain sedimentation ages: To what extent are volcanism and sedimentation synchronous?

Camille Rossignol, Erwan Hallot, Sylvie Bourquin, Marc Poujol, Marc Jolivet, Pierre Pellenard, Céline Ducassou, Thierry Nalpas, Gloria Heilbronn, Jianxin Yu, et al.

▶ **To cite this version:**

Camille Rossignol, Erwan Hallot, Sylvie Bourquin, Marc Poujol, Marc Jolivet, et al.. Using volcaniclastic rocks to constrain sedimentation ages: To what extent are volcanism and sedimentation synchronous?. Sedimentary Geology, 2019, 381, pp.46-64. 10.1016/j.sedgeo.2018.12.010 . insu-01968102

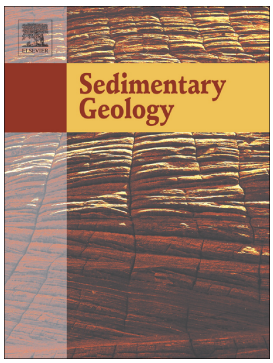
HAL Id: insu-01968102
https://insu.hal.science/insu-01968102

Submitted on 2 Jan 2019

HAL is a multi-disciplinary open access archive for the deposit and dissemination of scientific research documents, whether they are published or not. The documents may come from teaching and research institutions in France or abroad, or from public or private research centers.

L'archive ouverte pluridisciplinaire **HAL**, est destinée au dépôt et à la diffusion de documents scientifiques de niveau recherche, publiés ou non, émanant des établissements d'enseignement et de recherche français ou étrangers, des laboratoires publics ou privés.

Accepted Manuscript



Using volcaniclastic rocks to constrain sedimentation ages: To what extent are volcanism and sedimentation synchronous?

Camille Rossignol, Erwan Hallot, Sylvie Bourquin, Marc Poujol, Marc Jolivet, Pierre Pellenard, Céline Ducassou, Thierry Nalpas, Gloria Heilbronn, Jianxin Yu, Marie-Pierre Dabard

PII: S0037-0738(18)30284-7
DOI: https://doi.org/10.1016/j.sedgeo.2018.12.010
Reference: SEDGEO 5431

To appear in: *Sedimentary Geology*

Received date: 4 October 2018
Revised date: 25 December 2018
Accepted date: 26 December 2018

Please cite this article as: Camille Rossignol, Erwan Hallot, Sylvie Bourquin, Marc Poujol, Marc Jolivet, Pierre Pellenard, Céline Ducassou, Thierry Nalpas, Gloria Heilbronn, Jianxin Yu, Marie-Pierre Dabard , Using volcaniclastic rocks to constrain sedimentation ages: To what extent are volcanism and sedimentation synchronous?. Sedgeo (2018), https://doi.org/10.1016/j.sedgeo.2018.12.010

This is a PDF file of an unedited manuscript that has been accepted for publication. As a service to our customers we are providing this early version of the manuscript. The manuscript will undergo copyediting, typesetting, and review of the resulting proof before it is published in its final form. Please note that during the production process errors may be discovered which could affect the content, and all legal disclaimers that apply to the journal pertain.

ACCEPTED MANUSCRIPT

Using volcaniclastic rocks to constrain sedimentation ages: to what extent are volcanism and sedimentation synchronous?

Camille Rossignol[a]*, Erwan Hallot[b], Sylvie Bourquin[b], Marc Poujol[b], Marc Jolivet[b], Pierre Pellenard[c], Céline Ducassou[b], Thierry Nalpas[b], Gloria Heilbronn[d], Jianxin Yu[e], Marie-Pierre Dabard[b†]

[a]*Universidade de São Paulo, Departamento de Geofísica, Instituto de Astronomia, Geofísica e Ciências Atmosféricas – Rua do Matão, 1226 - Cidade Universitária, Butantã – 05508-090 São Paulo – SP, Brazil*

[b]*Univ Rennes, CNRS, Géosciences Rennes - UMR 6118, F-35000 Rennes, France*

[c]*Biogéosciences UMR uB/CNRS 6282, Université Bourgogne Franche-Comté, 21000 Dijon, France*

[d]*CASP, West Building, Madingley Rise, Madingley Road, Cambridge, CB3 0UD, United Kingdom*

[e]*State Key Laboratory of Biogeology and Environmental Geology, China University of Geosciences, Wuhan 430074, People's Republic of China.*

[†]*Deceased*

camil.rossignol@gmail.com; erwan.hallot@univ-rennes1.fr; sylvie.bourquin@univ-

ACCEPTED MANUSCRIPT

rennes1.fr; marc.poujol@univ-rennes1.fr; marc.jolivet@univ-rennes1.fr; pierre.Pellenard@u-bourgogne.fr; celine.ducassou@gmail.com; thierry.nalpas@univ-rennes1.fr; gloria.heilbronn@casp.cam.ac.uk; yujianxin@cug.edu.cn

**Corresponding author: Camille ROSSIGNOL (camil.rossignol@gmail.com)*

ACCEPTED MANUSCRIPT

Abstract

Volcaniclastic rocks are commonly used to date sedimentary series since absolute ages are routinely obtained from several geochronological methods. In this work, we present five selected geochronological studies (U-Pb on zircon) on late Paleozoic to Mesozoic volcaniclastic series from Asia, with the aim of discussing if absolute ages obtained on volcaniclastic rocks can be used directly to date sedimentation. For all these volcaniclastic series, volcanism and sedimentation are reputedly coeval and zircon grains have been dated to obtained depositional ages. Nevertheless, among the five volcaniclastic series, only two provide U-Pb/zircon ages that are demonstrably representative of the sedimentation ages (Guandao Section, south China, and Luang Prabang Basin, Laos). In the three other series (Wusu Section, northwest China, Chahe and Daxiahiou sections, south China), U-Pb/zircon ages are not suitable to constrain depositional ages. Perhaps more troubling, all the zircon grains collected from a volcanic layer in the Wusu Section are shown to exhibit ages that are much older than the sedimentation age of the deposits in which the volcanic layer is interbedded.

These five examples highlight two prerequisites that must be fulfilled in order to date the deposition of volcaniclastic sediments using geochronological methods: (i) at

ACCEPTED MANUSCRIPT

least some of the dated minerals must have crystallized during or just before one of the last eruptions that provided the volcaniclasts, and (ii) volcanic activity and sedimentation must have been coeval. Accurate sedimentation ages from radiometric dates can only be assessed if these prerequisites are fully demonstrated. A reliable method to verify this consists in systematically comparing the maximum depositional ages obtained from a set of samples along a section with their relative position in the section. Indeed, maximum depositional ages getting younger upwards in a section likely demonstrate that the volcaniclasts were produced during sedimentation and contain grains that crystallized immediately before each eruption. In such conditions, orders of magnitude for time scales of reworking can be estimated. They relate to the episodic and different rates of development of the volcanic edifices and fields, competing with the time necessary for erosion, transport and sedimentation.

Keywords

Volcaniclastic rocks; U-Pb zircon geochronology; Lag-time; Reworking time scale; Chronostratigraphy

1. Introduction

In volcanic environments, the products of volcanic activity can undergo various processes of volcanic (vesiculation, fragmentation, eruption, degassing, thermal fissuring, hydrothermalism), sedimentary (chemical weathering and mechanical erosion, transport, deposition, diagenesis) and/or tectonic (faulting) nature, all contributing to produce clasts. Along active-volcano slopes and in downstream sedimentary basins, particles of volcanic origin (volcaniclasts) accumulate (Fig. 1), and

ACCEPTED MANUSCRIPT

may be mixed in various proportions with "background" sedimentary particles (epiclasts), resulting in singular sedimentary rocks termed "volcaniclastic rocks". Primary volcaniclastic rocks, such as pyroclastic deposits, comprise unreworked volcaniclasts, whereas secondary volcaniclastic rocks are constituted by reworked volcaniclasts (White and Houghton, 2006). The diversity of volcanic rocks on Earth, the variety of eruption types (e.g., fragmentation styles of magma), along with the range of mingling processes between magma and sediments (e.g., Jerram and Stollhofen, 2002; Galerne et al., 2006; Martin and Nemeth, 2007), or mixing between volcaniclasts and epiclasts through erosional, transport, weathering and diagenetic processes (e.g., Huff, 2016; Zhu et al., 2017; Hong et al., 2018) can produce a very large variety of volcaniclastic rocks.

Volcaniclastic rocks are estimated to roughly represent one quarter of the total volume of sedimentary rocks deposited on Earth (Fisher and Schmincke, 1984). This relative proportion might be underestimated, as an unknown amount of fine-grained volcaniclastic rocks, commonly altered into clay, are often classified as shales (Fisher and Schimcke, 1984; Ver Straeten, 2004). Regardless of the exact volume of volcaniclastic rocks deposited on Earth, they predominated during the Paleoarchean (Eriksson et al., 2005; Ernst, 2009) and represent a major input in sedimentary systems throughout geological times (Ronov, 1972; Ross et al., 2005; Ernst, 2009).

In addition to their volumetric importance, volcaniclastic rocks and particles carry valuable information to reconstruct the magmatic history and the evolution of any given area (e.g., Lenhardt et al., 2011; Mattioli et al., 2012; Yang et al., 2012; Gao et al., 2013; Huff, 2016; Roverato et al., 2017; Hong et al., 2018). Indeed, because they often represent topographic highs, volcanic edifices may be rapidly eroded and sometimes, only the resultant volcaniclastic rocks may preserve relevant magmatic information.

ACCEPTED MANUSCRIPT

Furthermore, *in situ* lava flows (or *in situ* well-characterized pyroclastic deposits), interbedded within sedimentary layers, are relatively scarce in the sedimentary record. In contrast, reworked volcaniclasts, directly sourced by volcanic eruptions or by the erosion of volcanic rocks, accumulate in basins and are much more common in the sedimentary record (e.g., Turbeville, 1991; Lenhardt et al., 2011).

Volcaniclasts, occurring either as polyphazed rock fragments (glass ± crystals ± vesicles) or as individual fragments made by a single phase (glass or crystal), commonly contain minerals suitable for radiometric dating, such as zircon. Consequently, volcaniclastic rocks are widely used to provide radiometric ages for sedimentary series and/or to calibrate the temporal extent of fossils (biozones) and generate chronostratigraphic charts (e.g., Lehrmann et al., 2006; Ovtcharova et al., 2006; Yu et al., 2008; Shen et al., 2011; Blanchard et al., 2013; Rubidge et al., 2013; Gastaldo et al., 2015; Metcalfe et al., 2015; Schoene et al., 2015; Baresel et al., 2017). However, linking a radiometric age obtained from a volcaniclastic rock with the age of sedimentation is not straightforward. Lack of rigor in data interpretation may lead to misinterpretation of the real age of the volcaniclastic rocks, and therefore to interpret maximum depositional ages as sedimentation age (e.g., Young, 2014).

Assessing the contemporaneity between volcanism and sedimentation is intrinsically related to the definition and the classification schemes available for volcaniclastic rocks, which have been both debated for decades (e.g., Honnorez and Kirst, 1975; Orton, 1996; Busby, 2005; White and Houghton, 2006; Waitt, 2007; Manville et al., 2009, and references therein). These debates are rooted in the complexity of the volcaniclastic processes themselves (e.g., Manville et al., 2009), but also in the difficulty of demonstrating the contemporaneity between volcanic activity and sedimentation. For instance, Orton (1996, pp. 521) proposed to define “syn-eruptive deposits” as “a direct

ACCEPTED MANUSCRIPT

consequence of volcanic eruption. They [the syn-eruptive deposits] include not only volcanic and contemporaneous sedimentary processes during the eruption but also penecontemporaneous sedimentary processes following volcanism". Such a definition presents the advantage to be broad enough to include rocks that were formed under the direct influence of volcanic activity, but becomes ambiguous with the notion of "penecontemporaneity", as the time lapse between eruption(s) and sedimentation is not clearly defined. Additionally, it is notoriously difficult to establish that volcanic eruptions and sedimentation were contemporaneous in ancient and/or in poorly exposed volcano-sedimentary systems (e.g., Turbeville, 1991; Clayton et al., 1996; Orton, 1996; d'Atri et al., 1999; Bull and Cas, 2000; Sohn et al., 2008; Bernard et al., 2009; Cassidy et al., 2014; Moorhouse and White, 2016; Roverato et al., 2017). Attempts to establish differences between primary and secondary volcaniclastic rocks require identification of the genetic processes responsible for the formation of the volcaniclasts. Such identification is often ambiguous or even impossible, especially for ancient volcaniclastic deposits (Waitt, 2007).

To assess when volcaniclastic rocks can be used to constrain sedimentation ages, in the present work we explore the significance of radiometric ages obtained on minerals assumed to be volcanic in origin. We specifically focus on U-Pb dating on zircon, because of the ubiquity of this mineral in volcaniclastic rocks and the relative ease to obtain U-Pb zircon ages with reasonable precision and accuracy (e.g., Gehrels, 2012). However, much of the following also applies to any other geochronological tools (e.g., K-Ar and $^{40}Ar/^{39}Ar$ method on plagioclase; Marzoli et al., 2011; U-Th/He on zircon; Saylor et al., 2012; von Eynatten and Dunkl, 2012) and/or minerals (e.g., apatite; Chew et al., 2011), as long as these systems were not affected by subsequent geologic events.

ACCEPTED MANUSCRIPT

A few critical examples, selected from the literature and complemented by new data, are used to illustrate what can (and in some cases, what cannot) be inferred from the dating of volcaniclastic rocks. Although much of the issues raised by the dating of such rocks have been addressed in previous studies (e.g., Lehrmann et al., 2006; Lexa et al., 2010; Saylor et al., 2012; Wotzlaw et al., 2014), the present work attempts to present them in a coherent workflow combining field and analytical data in order to reduce mis- and over-interpretation of obtained ages.

2. Terminology

2.1. Volcaniclastic rocks terminology

The terminology currently used to classify volcaniclastic rocks relies primarily on the origin and depositional mechanisms of the particles that compose them (e.g., White and Houghton, 2006). The two main components occurring in volcaniclastic rocks are volcaniclasts and "background" detrital clasts. The terminology applied to the particles that are volcanic in origin may be confusing, especially for dating purposes. Indeed, the word "volcaniclast" may apply to any particle fragmented by a volcanic action, and are commonly named according to the mechanism of fragmentation. Clasts produced by explosive eruptions are referred to as pyroclasts, and are further subdivided into juvenile (derived directly from erupting magma), lithic (formed by the fragmentation of pre-existing rock) and composite (formed by mingling of magma with a clastic host) types (White and Houghton, 2006). The main other types of volcaniclasts are hydroclasts that form by magma-water interaction, and autoclasts produced by mechanical friction of moving lavas (e.g., Orton, 1996). Volcaniclasts may therefore be

ACCEPTED MANUSCRIPT

used to describe particles of different origins (both in terms of age and provenance) found in the same volcaniclastic rock, including volcanic but also non-volcanic ones.

Different definitions have also been proposed for the epiclastic particles. Epiclasts are sometimes defined as reworked fragments of volcanic origin (e.g., Fisher and Schmincke, 1984). In other studies, "epiclast" is used to refer to any particle deposited by "normal" sedimentary processes, irrespective of the origin of the clasts (e.g., Schmid, 1981; Orton, 1996), which may or may not be specified ("volcanic" or "non-volcanic" epiclasts; Schmid, 1981).

To avoid a definition requiring an *a priori* knowledge of the processes accounting for the formation of the volcaniclasts, we hereafter use a definition partly derived from the one of Le Maitre et al. (2002, after Schmid, 1981) for pyroclastic and mixed pyroclastic-epiclastic deposits (Table 1). However, in order to be as descriptive as possible, and following Best and Christansen (2001, after Fisher and Smith, 1991), we use the term "volcaniclast", instead of "pyroclast". Indeed, Le Maitre et al. (2002) define a "pyroclast" as a particle that has not been reworked. As the reworked character of a clast is difficult to assess, especially in ancient and/or poorly exposed deposits, a strict application of Le Maitre et al.'s (2002) nomenclature may be tendentious. Thus, the term "volcaniclast", here defined as any fragment (rock or individual crystal) of volcanic origin (whatever its shape and weathering), is preferred, unless the pyroclastic nature of the deposit can be confidently established. Any fragment exhibiting a non-volcanic texture (i.e., that of an intrusive, a metamorphic or a sedimentary rock) is hereafter considered as an epiclastic particle.

Importantly for dating purposes, the present definition makes no assumption regarding the contemporaneity between volcanic activity and sedimentation. Consequently, any sedimentary rock made up of at least 25 vol. % volcaniclasts is

ACCEPTED MANUSCRIPT

considered as volcaniclastic, even though the volcanism may significantly predate deposition of the sediments. Our definitions herein diverge from other classification schemes that require that volcanic activity and deposition of volcaniclasts were coeval (e.g., Orton, 1996; White and Houghton, 2006).

2.2. Volcaniclastic minerals terminology

Crystals from the same mineral species found in a volcaniclastic rock can have different origins and sources. Because of their ubiquity in various rocks and their ability to survive numerous sedimentary (e.g., Fedo et al., 2003; Thomas, 2011) and/or orogenic (e.g., Yakymchuk and Brown, 2014) cycles, zircon crystals provide a typical example of such minerals. Individual crystals enclosed within epiclasts are hereafter referred to as *epicrysts*, and different zircon epicryst populations may coexist in epiclasts. In addition, because of different histories and conditions for the melts residing in the magmatic plumbing system, volcaniclasts can also contain different populations of zircon grains (e.g., Charlier et al., 2005; Davidson et al., 2007; Miller et al., 2007; Bahlburg and Berndt, 2016).

Among the minerals contained in volcaniclasts, the *autocrysts* have to be distinguished from the *antecrysts*. The *autocrysts* correspond to the crystals that directly crystallized from the magma just before a given eruption (Davidson et al., 2007; Miller et al., 2007). The *antecrysts* are older than the *autocrysts* and crystallized during an earlier evolution stage of the same magmatic system. They have therefore been incorporated into the host magma before eruption (Davidson et al., 2007; Miller et al., 2007). In this context, the more common term *xenocrysts* refer to the crystals that were incorporated into the magma by assimilation of its surrounding host rocks (e.g., Best and Christansen,

ACCEPTED MANUSCRIPT

2001). The *inherited* grains are different, as they are defined as grains that underwent at least one anatexis episode of the magma source rock (Harrison et al., 1987, and references therein; Miller et al., 2007). It is also relatively common that a zircon grain exhibits a complex zoning and/or a core-rim texture (e.g., Pidgeon et al., 1992; Corfu et al., 2003, and references therein), exposing different domains that recorded different geologic events with different ages. For a volcaniclastic zircon grain in unmetamorphosed deposits, a rim overgrowth can typically be interpreted as the autocrystic domain, while the core may witness an antecrystic, xenocrystic or inherited history.

These notions of auto-, ante-, xenocrysts and inherited grains are only relative as they refer to the time of a specific magmatic event (a given volcanic eruption for our purpose). However, individual volcanoes as well as volcanic fields generally remain active over periods of several million years as magmatic systems are built by multiple increments (e.g., de Saint Blanquat et al., 2011, and references therein). Therefore, the host rocks for the last magmatic increments may correspond to earlier intrusions or volcanic deposits, such that the distinction between xenocrysts and antecrysts can be difficult to achieve (Miller et al., 2005). As exemplified later it may also be difficult to distinguish autocrysts from antecrysts (see also Miller et al., 2007).

2.3. Geochronological terminology and concepts

In recent years, a distinction has been made between a *date* and an *age*. A *date* corresponds to a number, expressed in years, directly calculated from an isotopic radioactive parent/radiogenic daughter ratio using the corresponding decay equation (Schone et al., 2013; Horstwood et al., 2016, and references therein). This *date* becomes

ACCEPTED MANUSCRIPT

an *age* only if geological significance (magmatic, metamorphic, hydrothermal, etc.) is given to it. Therefore, in some cases, a *date* can remain a *date* (i.e., with no meaning) if no logical explanation can be proposed for its significance (Horstwood et al., 2016). In some publications, a date can also be referred to as an *apparent age*.

A radiometric age, in an igneous context, corresponds to the time when a mineral cooled down below the so-called closure temperature (Dodson, 1973), except if this mineral was formed at a temperature lower than its closure temperature, in which case the obtained date corresponds to the time when the grain crystallized. This closure temperature is the temperature when there is no more significant diffusion of the isotopes out of the system. For a given geochronometer (U-Pb, Rb-Sr, K-Ar, etc.), each mineral bears its own closure temperature. In pristine (non-metamict) zircon grains of typical size (up to a few mm), the closure temperature for the U-Pb system is above 900°C (Cherniak and Watson, 2001), often significantly above magma solidus temperatures. For volcanic rocks, due to the rapid cooling of the lava, geochronological systems exhibiting low closure or annealing temperatures (e.g. U-Th/He on zircon; Saylor et al., 2012) can also be used to date an eruption.

Given the high closure temperature of the U-Pb system in zircon, the dates calculated from U-Pb isotope ratios in zircon grains are commonly interpreted as zircon crystallization ages. Such a high closure temperature implies that inherited or xenocrysts zircon grains incorporated in the magma are generally not reset and preserve their crystallization age. Besides, if a rim crystalizes onto the xenocrystic core of a zircon grain, the rim and the core record distinct geological events, resolvable by *in situ* analyses (e.g., Zimmermann et al., 2018, and references therein).

In sedimentary rocks (including volcaniclastic rocks), the date given by the youngest zircon population is referred to as a *maximum depositional age* (e.g., Fedo et al.,

ACCEPTED MANUSCRIPT

2003; Dickinson and Gehrels, 2009; Spencer et al., 2016, and references therein). Such an age has to be considered as maximum, since the zircon grains crystallized before their incorporation into the volcaniclastic rocks. Thus, the U-Pb ages obtained from zircon grains are older (if the system effectively remained closed, without subsequent Pb loss) than the real sedimentation ages of the deposits containing them.

3. Assessing the contemporaneity between volcanism and sedimentation

3.1. Sedimentological analyses

Classical sedimentological analyses, from outcrop to hand sample scale, constitute the first step to document the presence and the potential reworking of volcaniclastic particles. Such analyses involve the reconstruction of depositional environments by sedimentary facies analyses. Petrographic analyses further document the diversity, relative proportions, shapes and weathering of the volcaniclastic and epiclastic components that may help to establish the potential reworking of the volcaniclasts. Contemporaneity between volcanism and sedimentation is straightforward to infer when, for instance, interbedded lava flows or pyroclastic deposits, angular volcaniclasts, volcanic bombs and/or volcanic glassy shards are clearly identified. Conversely, well-rounded volcaniclasts usually suggest reworking (e.g., Sohn et al., 2008). It should be stressed that because volcanic edifices are subjected to erosion as they build up, evidence for reworking of the volcaniclasts is not necessarily a definitive argument to consider that volcanism and sedimentation were diachronous.

Assessing the potential reworking of the material composed of fine-grained volcaniclastic rocks (tuffaceous siltstone and tuffaceous mudstone; Table 1) is

ACCEPTED MANUSCRIPT

challenging (e.g., Clayton et al., 1996; Cassidy et al., 2014). Different approaches, relying on scanning and transmission electron microscopy (e.g., Clayton et al., 1996), magnetic susceptibility and color spectrophotometry analyses (Cassidy et al., 2014) coupled with geochemical investigations (Clayton et al., 1996; Wray and Wood, 1998; Yu et al., 2007; Cassidy et al., 2014; Hong et al., 2018) have been employed. As weathering and diagenesis quickly convert volcanic ashes into clay minerals, X-ray diffraction (XRD) analyses on the bulk and clay size fraction constitute an essential tool to assess the volcanic or epiclastic origin of a given claystone (e.g., Clayton et al., 1996; Pellenard et al., 2003; Spears, 2012; Deconinck et al., 2014; Huff, 2016; Pellenard et al., 2017; Hong et al., 2018). As diagenetic reactions not only depend on the chemical composition of the parent material (volcanic ashes) and the diagenetic grade, but also on the various physical and chemical conditions to which the volcanic ashes were subjected, a large variety of clay minerals can form (e.g., Hong et al., 2018; Gong et al., 2018). Devitrication of volcanic ashes during the early stages of diagenesis generally produces smectite, forming bentonite deposits in basic marine environments, where ionic activity is high (e.g., Fisher and Schmincke, 1984; Pellenard et al., 2003; Huff, 2016). In well-drained, acidic, continental environments, devitrification of volcanic ashes generally produces kaolinite, forming tonstein deposits (e.g. Bohor and Triplehorn, 1993; Spears, 2012; Pellenard et al., 2017). During burial diagenesis, smectite progressively transforms into illite/smectite mixed-layers (IS) through the addition of non-exchangeable K^+ ions forming rocks called K-bentonites (Huff, 2016). In terrestrial, coal-forming environments, kaolinite from tonstein can recrystallize into illite and chlorite (e.g., Admakin, 2002). Assessing the potential volcanic origin of a given claystone layer thus requires analysis of several samples throughout a sedimentary section in order to

ACCEPTED MANUSCRIPT

distinguish the epiclastic from the volcaniclastic clay layers (e.g., d'Atri et al., 1999; Deconinck et al., 2014; Pellenard et al., 2017).

3.2. Maximum depositional ages and statistical representativeness of a dataset

As for any type of *age*, a maximum depositional age is the interpretation of a *date* that, in order to be robust, requires the acquisition of several analyses. Out of all the analyses, this maximum deposition age is calculated using the youngest dates. Generally, a single analysis can only be considered as a date (or an apparent age) while several analyses are required to define an age (e.g., weighted averages). A minimum of 3 different dates obtained on distinct zircon grains overlapping in age at 2σ has been demonstrated to produce statistically robust maximum depositional ages (Dickinson and Gehrels, 2009). The use of distinct individual grains reduces the risk of relying on data obtained on a single exotic contaminant grain recovered during sample processing. An alternative approach consists in calculating a maximum depositional age from repeated analyses of the youngest grain (Spencer et al., 2016), or in the youngest domain of a grain, usually its rim (e.g., Zimmermann et al., 2018). This requires *in situ* analyses such as Laser Ablation – Inductively Coupled Plasma – Mass Spectrometry (LA-ICP-MS) or Secondary Ionization Mass Spectrometry (SIMS). To ensure that the youngest grain is not a contaminant, reproducibility from a separate aliquot is then required (Spencer et al., 2016).

As maximum depositional ages are calculated from analytical measurements, uncertainties are associated with the obtained ages (e.g., Schoene et al., 2013). For U-Pb ages on zircon, typical relative uncertainties, at the 2σ level, are of ca. 1-2% using LA-ICP-MS (e.g., Tiepolo, 2003; Schaltegger et al., 2015), or SIMS analyses (e.g., Schaltegger

ACCEPTED MANUSCRIPT

et al., 2015). They drop below 0.1% using Chemical Abrasion – Isotopic Dilution – Thermal Ionization Mass Spectrometry (CA-ID-TIMS, hereafter abbreviated CA-TIMS) and appropriate spikes (e.g., Mattinson, 2005; Schaltegger et al., 2015), although this method does not allow for in situ analyses as the whole grain is digested into hydrofluoric acid.

In a volcaniclastic sample, distinct populations of zircon grains (auto-, ante-, xeno-, epicrysts and inherited grains), or distinct domains within an individual grain, may be present, with very different relative proportions. Therefore, some of these populations may be missing from the data set because of the sampling techniques used to select the grains (handpicking for instance). As the representativeness of a dataset is not a linear function of the number of analyzed grains (Vermeesch, 2005; Andersen, 2005), it is difficult to estimate how representative a dataset is from the number of analyzed grains only. However, detection limits, which represent the relative proportions of a zircon population that is likely to remain undetected, can be calculated for a given sample (assuming a random sampling of the grains; Andersen, 2005). Detection limits provide straightforward means to assess the representativeness of a dataset. Their values depend on a chosen confidence level; usually the 50% and 95% confidence levels are quoted (Andersen, 2005). In this work, detection limits will be provided for datasets that have been filtered in order to eliminate analyses evidencing subsequent perturbations of the isotopic systems. For the U-Pb system, the relevant dataset corresponds to analyses concordant above a given threshold (e.g., Zimmermann et al., 2018, and references therein).

Statistically, to produce robust maximum depositional ages, repeated analyses are required (at least 3 analyses on 3 distinct crystals; Dickinson and Gehrels, 2009). Figure 2 gives the detection limits for 3 grains at the 50% and 95% confidence levels

ACCEPTED MANUSCRIPT

(Rossignol et al., 2016; see also Appendix A for further developments). Used for U-Pb dating on zircon, such a graph indicates that there is a 50% chance to sample at least 3 grains belonging to a population representing only 5% of the total zircon content from a dataset comprising 54 concordant grains (Fig. 2). To reach a 95% chance to sample at least 3 grains of such population, the dataset should comprise 124 concordant grains (Fig. 2). To obtain a geologically relevant maximum depositional age, this illustrates the necessity to analyze a large number of grains, especially when the youngest population exhibits a low relative proportion (as low as 0.25% in some volcaniclastic rocks, e.g., Burgess and Bowring, 2015).

3.3. Comparison between relative sedimentation ages and maximum depositional ages

The comparison between sedimentation age and maximum depositional ages of a set of samples can result in different cases (Fig. 3). Each of these cases has contrasted implications regarding the interpretation of maximum depositional ages.

In the first case (Fig. 3A), maximum depositional ages are getting younger together with sedimentation ages, upwards in a normal volcaniclastic succession. This trend indicates that the maximum depositional ages give a fair estimate of sedimentation ages, because both of the aforementioned assumptions are fulfilled (Fig. 3A'). Such volcaniclastic rocks are usually characterized by volcaniclasts displaying limited evidence of reworking and homogeneous textures.

In the second case (Fig. 3B), maximum depositional ages are getting older while the relative sedimentation ages get younger. Such an inverse correlation indicates that an older volcanic edifice (or complex) containing autocryst zircon grains, was progressively eroded as sedimentation proceeded. Contemporaneity between volcanic

ACCEPTED MANUSCRIPT

activity and sedimentation can clearly be ruled out and the maximum depositional ages are likely much older than the actual sedimentation age.

In the third case (Fig. 3C), all the obtained maximum depositional ages in the volcaniclastic succession are comparable within uncertainties. Such a situation may result from one or more of the following causes (assuming the maximum depositional ages derive from autocrysts):

- uncertainties on the ages are too large,
- stratigraphic distances between the collected samples are too short and/or sedimentation rates were too high with respect to the precision obtained for the maximum depositional ages,
- volcanism and sedimentation were not coeval, i.e., the different volcaniclastic layers originate from a unique, older volcanic edifice or layer.

The third case (Fig. 3C) may of course also occur when autocrysts are missing in the youngest volcaniclastic layers, either because the magma composition just before the eruption prevented zircon crystallization, or because of sampling bias (Fig. 2, e.g., sampled zircon populations correspond to antecrysts).

In the last case (Fig. 3D), the maximum depositional ages are randomly distributed along the sedimentary sequence. Such a situation likely results from maximum depositional ages derived from zircon populations that are not autocrysts (relative to the last eruptive episode). This situation may occur because:

- volcaniclastic rocks enclose only xenocrysts, inherited and/or epiclastic zircon grains. If the volcaniclasts are devoid of autocrysts (or even antecrysts), the resulting maximum depositional ages are likely to be much older than the depositional age.

ACCEPTED MANUSCRIPT

- the autocrysts were missed due to an insufficient number of concordant analyses (Fig. 2),
- volcanism and sedimentation were not coeval.

Both cases 3C and D can originate from a volcanic activity that was significantly older than the sedimentation. Consequently, maximum depositional ages must be considered as maximum only, as they are not always equivalent to sedimentation ages.

4. Time scale of reworking

4.1. Definition and rationale

In areas subject to active volcanism, the products generated during eruptions are usually deposited after having been affected by a series of volcanic and sedimentary processes, which commonly occur simultaneously and continuously over time. For instance, pyroclastic flows and lahars constitute end-members of a complete spectrum of volcaniclastic-rich sediment gravity flows (e.g., Orton, 1996; Freundt, 2003; Manville et al., 2009, and references therein). When a pyroclastic flow enters a water body (lake, sea), volcaniclasts are transported, sorted and winnowed. The resulting deposits can exhibit mineralogical sorting (e.g., Clayton et al., 1996) and display sedimentary structures (e.g., hummocky cross-stratification, bioturbation; d'Atri et al., 1999), similar to those typically found in reworked volcaniclastic deposits (e.g., Bull and Cas, 2000). However, most of the volcaniclasts that compose such volcaniclastics rocks were never stored nor subsequently remobilized before being deposited, implying that some volcaniclastic deposits made up of reworked volcaniclasts can provide valuable age constraints. It is then necessary to evaluate the time span between the eruption and the

ACCEPTED MANUSCRIPT

deposition of volcaniclasts in their final position, hereafter referred to as the *reworking time scale* and defined as follow:

$$\Delta t = t_{volc} - t_{sed}$$

where Δt is the reworking time scale, t_{volc} is the age of the youngest volcanic activity recorded by a volcaniclastic sample and t_{sed} the sedimentation age of the sample (Fig. 4A).

As autocryst zircon grains crystallize only a few tens to hundreds kyr or less before eruption (Wotzlaw et al., 2014), maximum depositional ages obtained from autocrysts provide an effective estimate of t_{volc}. Indeed, such time lapses between crystallization and eruption are negligible relative to LA-ICP-MS and SIMS analytical uncertainties. It is also negligible relative to the uncertainties from high precision CA-TIMS analyses, but only for rocks older than 100 Ma (Wotzlaw et al., 2014). The reworking time scale applies to any volcaniclastic rocks, irrespective of the duration of reworking of the volcaniclasts up to their ultimate deposition (Fig. 4B).

4.2. Duration of reworking

Assessing the duration of reworking for a given volcaniclast requires defining the ages of both the volcanic activity and sedimentation. As seen above, t_{volc} can be inferred from the maximum depositional ages obtained by U-Pb dating of autocryst zircon. In contrast, t_{sed} is often more difficult to precisely estimate. An estimation of t_{sed} can nonetheless be obtained in a sedimentary sequence where the maximum depositional ages get younger upwards (Fig. 3A). In this case, the sedimentation age for each sample is constrained by two maximum depositional ages, i.e., that of the sample itself and that provided by the sample located immediately above. An ambiguity may arise from the use of maximum

ACCEPTED MANUSCRIPT

depositional ages only, as they may be significantly older than sedimentation (e.g., Andersen, 2005). However, it is unlikely that a positive correlation linking maximum depositional ages and relative sedimentation ages for several consecutive samples could occur if volcanic activity and sedimentation were diachronous. Therefore, the situation of Fig. 3A is suitable to give an estimate of sedimentation ages, as long as at least several (the more, the better) consecutive samples yield maximum depositional ages getting younger with the stratigraphy. The difference between two distinct maximum depositional ages from two successive samples in the volcaniclastic sequence can further provide an estimate of the reworking time scale (Fig. 5). The duration of the latter partly depends on the sampling strategy, and cannot be smaller than the uncertainties on the maximum depositional ages.

Inferences on the duration of reworking are complicated when two or more successive volcaniclastic samples yield maximum depositional ages overlapping within age uncertainties (Fig. 6). This can be the consequence of reworking durations much shorter than the age uncertainties (Fig. 6A). Alternatively, overlapping uncertainties can happen when a maximum depositional age is obtained from antecryst zircon grains (Fig. 6B), which can crystallize several Myr before the eruption (Miller et al., 2007). Another hypothesis to account for such overlapping uncertainties is that significantly different reworking durations were involved for each of the successive layers. This may induce a temporally-limited, inverse correlation between two successive maximum depositional ages and the corresponding relative sedimentation ages (Fig. 6C). Such an inversion is likely to occur in volcaniclastic successions derived from volcanic rocks with variable susceptibilities to mechanical erosion. For example, as any unconsolidated rock, a tephra layer may be easily eroded and reworked, while under the same environmental conditions, a massive lava flow, or a consolidated tuff, is more resistant to erosion. As a

ACCEPTED MANUSCRIPT

result, the volcaniclastic layers derived from the former will exhibit shorter reworking times than those deriving from the latter. Typically, composite stratovolcanoes, which are built up by alternating episodes of effusive and explosive eruptions, emit such products with different erodibilities. Their dismantling is thus likely to provide volcaniclastic successions characterized by temporally–limited time lapse showing maximum depositional ages getting older upwards (Fig. 6C), which may be common in the volcaniclastic rock records (e.g., Kataoka et al., 2009). These theoretical considerations illustrate the importance of analytical uncertainties in the dataset, not only to recognize syn-sedimentary volcanism (Fig. 3), but also to evidence that reworking durations may significantly vary among the volcaniclastic layers forming a single sedimentary succession.

4.3. Strategies to obtain reworking time scales

In volcaniclastic successions where maximum depositional ages overlap (Fig. 3C), it is not possible to infer a sedimentation age (Fig. 6). It is therefore important to minimize the uncertainties of maximum depositional ages, but also to adapt the sampling strategy to the sedimentation rate of the studied volcaniclastic succession.

Minimizing the uncertainties of maximum depositional ages can be achieved using the most accurate and precise analytical methods for radiometric measurements, which is the CA-TIMS method for U-Pb isotopic measurements on zircon grains. However, the CA-TIMS method does not allow for in situ analysis, requires important laboratory infrastructures (e.g., ultra-clean laboratory), is time consuming and expensive (e.g., von Eynatten and Dunkl, 2012), thus commonly providing far fewer analyses than if the measurements were performed using, for example, LA-ICP-MS.

ACCEPTED MANUSCRIPT

Generally, about 10 grains are analyzed by CA-TIMS while hundreds to thousands of grains can be dated using LA-ICP-MS (e.g., Pullen et al., 2014). A balance must thus be found between the goal of improving the precision of a given age and the necessity to analyze enough grains to effectively date the youngest zircon population from each sample. Indeed, if not enough grains are dated, the chance to miss a population, including the youngest one, is very high, especially if an age population is defined by only a few grains (Vermeesch, 2004; Andersen, 2005) (Fig. 2). However, this may be partly counterbalanced by the structure of zircon populations in most geodynamic settings where volcaniclastic rocks are common (Cawood et al., 2012). For example, the dominant zircon population in volcaniclastic rocks deposited in suprasubduction settings, such as foreland and backarc basins, is generally the youngest one (Cawood et al., 2012), thus maximizing the chance to sample the youngest population even when only a few grains are analyzed. Nonetheless, in some volcaniclastic rocks, autocrystic zircon populations can have very low relative abundances (e.g., as low as 0.25% in volcaniclastic rocks associated with the Siberian Traps; Burgess and Bowring, 2015), if not absent altogether. A suitable approach consists in screening the ages of a large number of detrital zircon grains using LA-ICP-MS dating. As this method is rapid and consumes only a limited amount of each crystal, it is thus possible, once the youngest concordant grains are identified, to analyze them again using CA-TIMS. Such an approach has been successfully applied to different rock types (e.g., Zakharov et al., 2017), including volcaniclastic rocks (Burgess and Bowring, 2015).

Another complementary strategy consists in adjusting field sampling to both the expected sedimentation rates and the analytical precisions. Ideally, for a ca. 100 Ma old volcaniclastic section deposited at a rate of ca. 100 m/Ma and that will be dated by LA-ICP-MS (1% relative precision), an appropriate sampling spacing is ca. one sample every

ACCEPTED MANUSCRIPT

one hundred meters. Using CA-TIMS (0.1% relative precision), a denser sampling (ca. one sample every ten meters) would result in smaller reworking durations. However, as sedimentation rates in volcaniclastic environments are highly variable, ranging from a few meters to thousands of meters per Ma (e.g., Allen et al., 2007; Xie and Heller, 2009; Blanchard et al., 2013), a pragmatic approach consists in undertaking a double sampling strategy, by collecting samples at two different stratigraphic scales (for example, 5 samples distributed along a 500 m-thick portion of the section, and 5 other samples distributed along a 50 m-thick portion of the section). Preliminary geochronological analyses, at first performed on a limited number of samples, may help to assess the best scale of investigation and select the appropriate samples. The preliminary results must then be confirmed by dating the other remaining samples collected at the appropriate stratigraphic scale.

5. Revised examples of dated volcaniclastic and volcanic sequences

To highlight the importance of verifying contemporaneity between volcanism and sedimentation as well as assessing the duration of the reworking of volcaniclasts, five examples, taken from late Paleozoic and early Mesozoic volcaniclastic rocks from Asia, are presented (Fig. 7). Four examples (Daxiakou, Chahe and Guandao sections, China, and the Luang Prabang Basin, Laos) are selected from the literature (Gao et al., 2013; Yu et al., 2008 and Shen et al., 2011; Lehrmann et al., 2006; and Blanchard et al., 2013 and Rossignol et al., 2016, cf. Appendix B). The fifth example consists of a newly acquired dataset (Wusu Section, China). X ray diffraction (XRD) analyses performed on the bulk rock and the clay-size fraction (<2 μm) on fine-grained volcaniclastic material (Appendix C) are provided to complement those available for the Chahe Section (Yu et al., 2008).

ACCEPTED MANUSCRIPT

New U-Pb zircon dating results are also presented (Appendices D and E) for the Chahe and Wusu sections.

There is a large number of studies from Asia using volcaniclastic rocks, because of the ubiquity of these rocks, especially in reference sections documenting the Permian-Triassic mass extinction and recovery in both marine and continental settings (e.g., Lehrmann et al., 2006; Yu et al., 2008; Shen et al., 2011; Baresel et al., 2017). Moreover, some of these sections were studied to provide time calibrations for the international chronostratigraphic chart (Cohen et al., 2013). Notably, the boundary between the Early and the Middle Triassic was calibrated using the dating results from the Guandao Section (Lehrmann et al., 2006). The selected examples cover different analytical techniques classically used to date zircon grains (ID-TIMS, including CA-ID-TIMS, and LA-ICP-MS). They also correspond to a wide range of depositional environments, including marine and terrestrial paleoenvironments. For consistency, all the maximum depositional ages were recalculated following the procedure described in Rossignol et al. (2016) from the published data compiled in Appendix B and from the new data available in Appendix E. The recalculated maximum depositional ages are identical, within uncertainties, to those reported in the original studies (except for example 1, for which no maximum depositional age is reported in the original study). All the uncertainties are quoted and depicted at the 95% confidence level (Table 2).

ACCEPTED MANUSCRIPT

5.1. Example 1: maximum depositional ages of the tuff layers in the marine "Permian-Triassic" Daxiakou Section, south China

To study the volcanism described as coeval with the Permian-Triassic mass-extinction event, Gao et al. (2013) undertook an integrated petro-geochemical and

ACCEPTED MANUSCRIPT

geochronological (LA-ICP-MS U-Pb dating on zircon) study of the volcaniclastic beds in the marine Daxiakou Section, south China, (Fig. 7) that is believed to span across the Permian-Triassic boundary. Ten clay layers, each being a few cm thick, of known stratigraphic positions, were collected along the ca. 2 m-thick section and dated (Fig. 8). The petrographic analyses performed on these samples indicate that the corresponding layers were, before alteration into clay, almost exclusively made up of volcanic, mostly dacitic, ashes (Gao et al., 2013). Maximum depositional ages, which were not calculated in the original work (Gao et al., 2013), are provided in Table 2.

Due to short stratigraphic distance between the sampled layers (a few dm, or less) and to the relative uncertainties on the ages (ca. 1 %), most of the obtained maximum depositional ages overlap (Fig. 8). The sample from the bottom of the section gives the youngest maximum depositional age (Early Triassic), which is, surprisingly, significantly different from the Permian to Triassic maximum depositional ages obtained from 2 samples (b264 and b266, Fig. 8) above in the section. Compared to the sedimentation ages, the maximum depositional ages do not get younger upwards in the section, as expected when volcanism and sedimentation are coeval (Fig. 3A). As a whole, they appear uncorrelated with the corresponding sedimentation ages (Fig. 3D) and, for some of the samples (b249, b259-b and b264, Fig. 8), maximum depositional ages are getting older upwards, suggesting reworking (Fig. 3B). In addition, five out of the six samples that were collected below the supposed Permian-Triassic boundary (Gao et al., 2013) give maximum depositional ages that are significantly younger (within uncertainties) than the age of the boundary (Burgess et al., 2014) (Fig. 8).

Such an erratic distribution of the maximum depositional ages could result from a sampling bias toward the youngest, autocrystic zircon populations in some of the samples, and especially in those yielding the oldest maximum depositional ages. Only a

ACCEPTED MANUSCRIPT

few Myr separate the oldest maximum depositional ages from the youngest. The former may thus have been derived from autocrysts from earlier eruptive episodes, or from antecrysts. Correspondingly, a few samples (e.g., b255) exhibit a range of individual concordant ages (Appendix B), indicating that the clay layers contain several distinct zircon populations. Also supporting the hypothesis of missing zircon populations in some of the samples are the relatively high values of the detection limits (the higher the values, the higher the chances to miss a population; Fig. 2). For the sample set, the detection limits for 3 grains range from 8.6% to 25.9% at the 50% probability level, and from 19.0% to 50.7% at the 95% probability level (Table 2). Autocrystic zircon crystals may thus be missing due to a sampling bias or due to their absence in the volcanic rock that produced some of the samples.

Despite the erratic distribution of the maximum depositional ages, the Daxiakou section may still have been deposited while volcanism and sedimentation were coeval, as assumed in previous studies (Gao et al., 2013). However, the geochronological data do not confirm, nor invalidate, this assumption (see Figs. 3D, 8). As such, the geochronological data obtained in the Daxiakou Section should be considered as maximum depositional ages and not as sedimentation ages. These maximum depositional ages also indicate that the deposition occurred after the Permian-Triassic transition (Fig. 8), ruling out the inferred contemporaneity of the marine Daxiakou beds with the Permian-Triassic mass extinction (Gao et al., 2013).

ACCEPTED MANUSCRIPT

5.2. Example 2: the terrestrial "Permian-Triassic" ash layers from the Chahe Section, south China

To investigate mechanisms that triggered the Permian-Triassic mass extinction, it is fundamental to assess the contemporaneity between the terrestrial and the marine extinction events (e.g., Twitchett et al., 2001; Shen et al., 2011; Gastaldo et al., 2015; Wang et al., 2018). For this purpose, reference outcrops in both the terrestrial and marine environments must be accurately dated. Among the presently known Permian-Triassic basins, only a few sections comprising volcaniclastic layers were deposited in a terrestrial setting. The Chahe Section, south China, (Fig. 7) is one of those.

Before the present work, two layers (each 10 to 15 cm-thick; beds 66 and 68; Fig. 9) interbedded in a ca. four m thick portion of the section (Fig. 9) were described as volcaniclastic (Yu et al., 2007; Gong et al., 2018, and complementary XRD analyses presented in the Appendix C). Reinvestigating the Chahe Section, we report a new volcaniclastic layer (bed 63; Fig. 9) made up of mainly R1-R3 type illite-smectite mixed-layer, with a characteristic mineralogy of K-bentonite (Appendix C). All together, these results suggest that the three claystone beds (beds 63, 66 and 68) likely correspond to weathered ash layers deposited subsequently to explosive volcanic eruptions, as established in the Chahe (Yu et al., 2007; Gong et al., 2018) and neighboring sections (Hong et al., 2018; Gong et al., 2018).

New LA-ICP-MS U-Pb geochronological analyses on zircon grains were performed on the newly identified volcaniclastic layer (bed 63, Fig. 9; Appendices D, E). Three samples collected within an overlying volcaniclastic bed (bed 68; Fig. 9) have already been dated by ID-TIMS (Yu et al., 2008) and high-precision CA-TIMS (with relative uncertainties as low as 0.03%; Shen et al., 2011) methods. The dating results obtained in these two studies yielded significantly different ages. As the detection limits for both

ACCEPTED MANUSCRIPT

studies are high (because of the use of TIMS methods), ranging from 8.3% for the $DL_{1(pL=0.5)}$ to 90.3% for the $DL_{3(pL=0.95)}$ (Table 2), the chances to have missed the youngest population are high. Consequently, we undertook new LA-ICP-MS analyses on zircon grains extracted from a fourth sample collected within the same bed (Appendices D, E), for which we obtained much lower detection limits, ranging from 1.9% for the $DL_{1(pL=0.5)}$ to 50.7% for the $DL_{3(pL=0.95)}$ (Table 2). In total, five samples have been dated in two volcaniclastic layers from the Chahe Section (Fig. 9).

Four out of the five maximum depositional ages overlap within uncertainties (Fig. 9). This makes the apparent distribution of these maximum depositional ages compatible with a volcanism coeval with sedimentation (see Fig. 3A), but the overlapping uncertainties and the limited number of volcaniclastic samples suggest an ambiguous situation (Fig. 3C, D). Indeed, there are, for now, only two beds yielding maximum depositional ages. Furthermore, some other comparable stratigraphic sections also located in the vicinity of Chahe, comprise volcaniclastic beds made up of reworked ashes (He et al., 2004; Hong et al., 2018). The occurrence of a significant proportion of antecrysts, and/or xenocrysts, and inherited and/or epicrystic zircon grains in at least one volcaniclastic layer (sample CH 68, this work, Appendices D, E), and the significantly different ages (within error) in bed 68 (Fig. 9) demonstrate a mixing of different zircon populations. These different populations could result from a significant reworking of the volcanic ashes before their final deposition for this sample. This is consistent with XRD results, which reveal that sample CH68 contains more vermiculite than CH63 (Appendix C). Vermiculite is not commonly associated with tonsteins or K-bentonite and could mark reworking and mixing of ashes with epiclastic background particles, as it is common in tuffites.

ACCEPTED MANUSCRIPT

It is not clear that the different ages obtained by U-Pb dating in claystone beds of the Chahe Section correspond to sedimentation ages, neither that the dated layers correspond to tuffs. As such, these ages should be considered as maximum depositional ages. Together with the fact that numerous faults affected this section (Bourquin et al., 2018a), the occurrence of only two dated layers explains why the exact location of the Permian-Triassic boundary in this section is still strongly debated (e.g., Shen et al., 2011; Yu et al., 2015; Zhang et al., 2016; 2018; Bourquin et al., 2018a, b; Wang et al., 2018). In this example, high precision dating (obtained by CA-ID-TIMS) is not sufficient in defining the actual sedimentation ages of the layers.

5.3. Example 3: reworking time scale for the tuff layers from the Early-Middle Triassic boundary in the marine Guandao Section, south China

Dating of the boundary between the Lower and the Middle Triassic is critical to understand the rate of recovery of the biosphere following the Permian-Triassic mass extinction (e.g., Chen and Benton, 2012). For that purpose, high precision ID-TIMS U-Pb dating on volcaniclastic rocks from the marine Guandao Section, south China (Fig. 7) was performed on zircon grains extracted from layers described as ash tuffs interbedded in between pelagic carbonates beds (Lehrmann et al., 2006). The dates obtained by Lehrmann et al. (2006) were interpreted as eruption ages, and therefore as depositional ages. Consistent with their relative stratigraphic positions below and above the Lower-Middle Triassic boundary, respectively, these ages were used to define the still accepted age of the boundary at 247.2 Ma by linear interpolation (Lehrmann et al., 2006; Cohen et al., 2013).

ACCEPTED MANUSCRIPT

The maximum depositional ages from the Guandao Section get younger together with their relative sedimentation ages (Fig. 10). The lowermost sampled beds, which are only 0.5 m apart, yield identical dates within uncertainties. Nevertheless, the overall trend between sedimentation and maximum depositional ages provides evidence for coeval sedimentation and volcanism, supporting the conclusions of Lehrmann et al. (2006). ID-TIMS analyses yielded 15 to 16 concordant grains per sample and relatively low detection limits, ranging from 4.2% for $DL_{1(pL=0.5)}$ to 36.4% for $DL_{3(pL=0.95)}$ (Table 2), suggesting that the youngest zircon populations were analyzed in each sample. Following Lehrmann et al. (2006), these populations possibly correspond to autocrysts from four successive eruptions and deposited, as time proceeded, within the pelagic succession. However, the two lowermost samples yield overlapping maximum depositional ages (Fig. 10). Consequently, it cannot be discarded that some zircon grains have been reworked from a slightly earlier eruption, or are in fact antecrysts minerals (see Fig. 6).

An estimate of the reworking time scale can be deduced from samples lying below and above the Lower-Middle Triassic dated to 247.26 ± 0.22 Ma and 246.82 ± 0.23 Ma, respectively (Table 2). Taking uncertainties into account, the reworking is constrained to be ≤ 0.89 Myr. Such a duration (0.89 Myr) should probably be considered as a safe uncertainty for the age of the boundary between the Lower and the Middle Triassic (247.2 Ma; Lehrmann et al., 2006; Cohen et al., 2013).

ACCEPTED MANUSCRIPT

5.4. Example 4: coeval volcanism and sedimentation in the terrestrial Triassic tuffitic series from the Luang Prabang Basin, Laos

The Luang Prabang Basin, located in Laos (Fig. 7), comprises a range of volcaniclastic rocks (e.g., Blanchard et al., 2013; Rossignol et al., 2016). A rich fossil record has been excavated in these rocks, documenting the dispersal of continental species and the Triassic recovery subsequent to the mass extinction that took place at the end of the Permian (Bercovici et al., 2012; Blanchard et al., 2013).

Most of the volcaniclastic rocks, deposited in alluvial to fluvial environments, display clear and unambiguous evidence for reworking, as shown by the occurrence of well-rounded volcanic boulders and trough cross bedding (Blanchard et al., 2013). Some layers contain almost exclusively volcaniclasts, many are volcaniclast-rich, while a few beds contain only a small proportion of volcaniclasts. The volcaniclastic rocks thus classify as tuffites and pyroclastic rocks (Blanchard et al., 2013; Rossignol et al., 2016). The nature of the volcaniclasts is rather homogeneous in each of the individual layers. Also noticeable is the occurrence of feldspar and apatite grains displaying angular shapes, despite the fact that these mineral species are prone to be easily rounded, or even destroyed, during transport (Morton and Hallsworth, 1999).

Maximum depositional ages for the five selected volcaniclastic samples were obtained using U-Pb LA-ICP-MS dating on zircon grains along a ca. 400 m thick succession (Blanchard et al., 2013; Rossignol et al., 2016) (Fig. 11). Although the oldest of the maximum depositional ages overlap, a comparison with the relative sedimentation ages shows that maximum depositional ages are getting younger upwards (Fig. 11), indicating that sedimentation and volcanism were coeval. The low detection limits, ranging from 1.7% for $DL_{1(pL=0.5)}$ to 38.6% for $DL_{3(pL=0.95)}$ (Table 2),

ACCEPTED MANUSCRIPT

suggest that the dominant populations, including the youngest ones, were effectively dated.

The overlapping ages possibly suggest that some of the layers contain autocrysts and that, therefore, some of the maximum depositional ages have been calculated from antecrysts (see Fig. 6B). In the present example, however, the volcaniclastic beds exhibit planar and trough cross stratification suggesting that the products of earlier eruptions may have been reworked and accumulated by pure sedimentary processes instead of resulting from direct volcanic eruptions (Blanchard et al., 2013; Rossignol et al., 2016). In such a case, the case presented in Fig. 6C fits the available dataset. The maximum durations of reworking that can be estimated using the non-overlapping ages range from 5.9 to 7.4 Myr (Fig. 11). However, the overlapping ages also indicate that much shorter durations could also be possible. Indeed, some andesitic to dacitic boulders collected within the tuffitic layers yielded ages significantly older than the maximum depositional ages of the tuffite deposits (Rossignol et al., 2016), indicating that the Luang Prabang tuffites consist of a mixture of dismembered lava flows and tephra layers. Because their erodibility is different, it can be expected that they provided different reworking time scales.

5.5. Example 5: coeval volcanism and sedimentation in the terrestrial Jurassic tuffs from the Wusu Section, northwest China

The Middle Jurassic Wusu Section from the southern Junggar Basin, northwest China (Fig. 7), contains several dm- to m-thick volcanic tuffs, interlayered with coal, sandstones and pebbly conglomerates, typical of alluvial plain deposits (Hendrix et al., 1992; Hendrix, 2000; Yang et al., 2013; Heilbronn, 2014). The thick tuff layers do not

ACCEPTED MANUSCRIPT

show direct evidence of reworking and, in some locations, plant remains are preserved (Fig. 12A). The layers contain a significant amount of angular quartz and few feldspars fragments as well as glassy to cryptocrystalline lapilli that may show fluidal textures. The mineralogical composition indicates the rhyolitic to dacitic nature of the layers. The sequence along the section is known to be Middle Jurassic (ca. 174.1 Ma to ca. 163.5 Ma; Cohen et al., 2013) in age (Tang et al., 2014, and references therein). The Middle Jurassic age of the section is well constrained from flora content (e.g., Li et al., 2014, and references therein).

One of these tuff layers was sampled for U-Pb dating on zircon grains (Appendices D, E). A total of 84 grains (84 analyses) were dated, among which 35 analyses are concordant, yielding fairly low detection limits, ranging from 2.0% for $DL_{1(pL=0.5)}$ to 17.0% for $DL_{3(pL=0.95)}$ (Table 2). Despite such low detection limits, poorly represented populations of grains could have been missed during grain sampling.

All the obtained individual zircon dates, ranging from ca. 960 to ca. 267 Ma, are significantly older than the Middle Jurassic age of the section (Fig. 12B). The youngest concordant grain gives a date of 267.3 ± 6.9 Ma (Appendix E) and the main mode in age distribution is centered at ca. 325 Ma (Fig. 12B). With no evidence for reworking in the volcanic layers, these zircon grains are interpreted as xenocrysts and/or inherited grains. Indeed, differences between the ages of volcanic eruptions and those of the dated zircon grains indicate that neither autocrysts nor antecrysts were sampled. This might relate to under-sampling (i.e., too few grains have been analyzed), a grain-size issue as the autocrysts might have been too small to be recovered from the crushed rock, or thermodynamical conditions preventing zircon crystallization in the magma prior to the eruption.

ACCEPTED MANUSCRIPT

Nevertheless, these data would allow an estimation of a maximum depositional age, which in this case, does not provide any new information. This example illustrates the importance of identifying the autocrysts for dating purposes in volcanic and volcaniclastic rocks.

6. Discussion: what can reliably be inferred from U-Pb dating of zircon grains from volcaniclastic rocks?

For any volcaniclastic rock, it is possible to provide an age approaching the actual depositional age only if it can be demonstrated that (i) the dated grains are autocrysts that crystallized in the magma a short time before the eruption and (ii) volcanism and sedimentation were coeval. As previously illustrated, both conditions must be achieved together, which is sometimes complex to demonstrate.

Volcanic rocks do not systematically contain autocrysts. Indeed, during their evolution, magmas are not permanently saturated in zirconium (Zr) to pertain zircon crystallization. Direct techniques to identify autocrysts assume that thermodynamical equilibrium is achieved between crystals and melts (e.g., Davidson et al., 2007). However, identifying different age populations of crystals in samples is a useful indirect means to evaluate if autocrysts are present. Indeed, discussing the potential autocrystic nature of the crystals becomes possible from a series of maximum depositional ages getting younger upwards, as it likely reflects the occurrence of autocrysts in the samples (e.g., Guandao Section, south China, and Luang Prabang Basin, Laos). On the contrary, autocryst-free volcaniclastic rocks likely result in an uncorrelated relationship between sedimentation and maximum depositional ages (e.g., Daxiakou and Chahe sections,

ACCEPTED MANUSCRIPT

south China). If the absence of autocryst is proven, absolute dating of the sedimentation using radiometric dating methods is impossible (e.g., Wusu Section, northwest China).

Contemporaneity between volcanism and sedimentation is also difficult to assess. This is especially true for ancient volcaniclastic rocks because field and/or petro-geochemical investigations give results that are often ambiguous regarding reworking. A peculiar attention must be paid when dealing with fine-grained volcaniclastic sediments (e.g., Clayton et al., 1996; Cassidy et al., 2014; Hong et al., 2018). In the Daxiakou and Chahe examples, the volcanic nature of the volcaniclasts is convincing, but the obtained maximum depositional ages cannot exclude that the volcaniclasts were reworked. Misidentification of the reworked nature of the volcaniclasts has evident consequences for the interpretation of dates obtained from geochronological analyses. Consequently, a date given by the youngest zircon population must only be considered as a maximum depositional age, which may differ markedly from the sedimentation age (e.g., Andersen, 2005). Intuitively, reworking is not expected to provide maximum depositional ages getting younger upwards in a section (Fig. 3B to D). However, such trend of ages getting younger upwards can also be preserved in the case of reworking, as exemplified by the volcaniclastic deposits from the Luang Prabang Basin. In such a case, it can therefore be assumed that the time scales of reworking were shorter than the time lapses separating successive eruptive events.

The absence of maximum depositional ages getting younger upwards in a section may indicate that sedimentation and volcanism were not coeval. It may also occur when volcanism and sedimentation were coeval, in which case the following additional reasons may be involved, assuming a sufficient number of available samples (≥3 samples required, 3 being the minimum required in order to identify any trend):

- unadapted dating method yielding age uncertainties that are too large;

ACCEPTED MANUSCRIPT

- inadequate field sampling strategy; samples were collected too close to each other;
- an insufficient number of zircon grains were analyzed (Vermeesch, 2004; Andersen, 2005) (Fig. 2; Appendix A).

For all the above-mentioned reasons, including the possible absence of datable autocrysts in some of the samples and the possible reworked nature of the volcaniclasts, it remains impossible to prove from the available datasets if volcanism and sedimentation were coeval.

When a volcaniclastic rock comprises autocrysts that were likely produced contemporaneously with sedimentation, a reworking time scale can be determined. Different orders of magnitude for the calculated reworking time scales are observed from the Guandao Section (south China) and the Luang Prabang Basin (Laos). They range from ca. 1 Myr for the former to ca. 7 Myr for the latter. These different orders of magnitude relate to source to sink sedimentary system issues. Upstream, the volcanic systems produce source materials at different rates (e.g., Manville et al., 2009) ranging from a few hours to a few million years. Upstream and downstream, erosion, transport and sedimentation also occur at different rates and time scales, which do not necessarily match those of the volcanic production. The interplay between these rates and time scales accounts for the characteristics of the volcaniclastic deposits downstream, and possibly for the different orders of magnitude of the reworking (Fig. 13).

Volcanic activity encompasses eruption events alternating with quiescent periods. These cycles may be periodic or aperiodic (e.g., Hildreth and Lanphere, 1994; Denlinger and Hoblitt, 1999) and occur over a range of time scales, or time units, lasting from hours (e.g., Voight et al., 1998; Turner and Costa, 2007; Michaut et al., 2013) to millions of years (Hildreth and Lanphere, 1994; Turner and Costa, 2007; de Saint Blanquat et al.,

ACCEPTED MANUSCRIPT

2011). They concern individual volcanoes (e.g., Voight et al., 1998), as well as larger volcanic fields or provinces (e.g., Lewis-Kenedi et al., 2005). Depending on the time scales of the cycles (eruptions and quiescent intervals), different volcaniclastic rock units (Fisher and Schmincke, 1984; Orton, 1996; Manville et al., 2009) can be defined downstream where the deposits are preserved (Fig. 13). The temporal link between volcanic activities and the corresponding rock units preserved in a basin is however not straightforward. Indeed, temporary storage before final deposition may increase reworking time scales, which also depend on the erodibility of the volcanic rocks and the transport distance between the source and the basin (e.g., Kataoka et al., 2009).

Different time scales of reworking may occur within the same volcaniclastic succession. This relates to complex facies associations and abrupt facies changes that commonly characterizes volcaniclastic depositional environments (e.g., Turbeville, 1991; Orton, 1996; Stow et al., 1998; Allen et al., 2007; Sohn et al., 2008, 2013; Kataoka et al., 2009; Manville et al., 2009; Lenhardt et al., 2011; Cutino and Scasso, 2013; Roverato et al., 2017). There is, however, no systematic correspondence between reworking time scales and volcano-sedimentary facies. For instance, volcaniclastic facies characterized by well-defined sedimentary structures (e.g., ripples marks) can be made up of volcaniclasts that were reworked for less than a month (Sohn and Yoon, 2010). Similar sedimentary structures and facies can also be characteristic of secondary volcaniclastic deposits with much longer reworking durations (e.g., Bull and Cas, 2000). The erodibility of the volcanic material plays also an important role in controlling these rates (i.e., Fig. 6C).

Although the relationships between time scales and the rock units as proposed by Manville et al. (2009) are not straightforward, an overall correspondence can be discussed, from the shortest (Fig. 13A) to the longest time scales (Fig. 13E). The shortest

ACCEPTED MANUSCRIPT

reworking time scales likely correspond to the erosion and (re)deposition of unconsolidated volcanic deposits. Time scales ≤ 1 Myr arguably characterize deposits resulting from the dismantling of a single volcanic layer (i.e., an eruption unit formed during a single eruption, as defined by Manville et al., 2009) (Fig. 13A) or that of several layers corresponding to an eruptive episode (Fig. 13B; episode unit). Each of the volcaniclastic layers from the Guandao Section (Lehrmann et al., 2006) likely correspond to such eruption or episode unit.

Volcaniclastic rocks characterized by longer reworking time scales (> 1 Myr) likely comprise reworked volcaniclasts that were produced by several successive eruption episodes from one or several volcano(es). Such volcaniclastic rocks consequently record period (Fig. 13C) or epoch (Fig. 13D) units. The volcaniclastic rocks from the Luang Prabang Basin (Blanchard et al., 2013; Rossignol et al., 2016) likely correspond to this type of deposits.

The longest reworking time scales (> 10 Myr) may indicate that sedimentation is much younger than volcanism and that all the volcaniclasts are reworked (Fig. 13E). In such a case, the epiclast/volcaniclast ratio is expected to be high. However, this ratio may also be low in specific geological contexts, where the erosion of an old volcanic province (e.g., a Large Igneous Province; see Sheth, 2007) constitutes the unique source of volcaniclasts in the basin. The resulting volcaniclastic rocks are then made up nearly exclusively by volcaniclasts, which are not contemporaneous with the eruptions (e.g., Shipboard Scientific Party, 2001; Ross et al., 2005; He et al., 2010). Integrated surveys of the regional geology are likely to provide clues to interpret the nature of the volcaniclastic deposits.

A flowchart describing the successive steps required to assess “how coeval volcanism and sedimentation were” is presented in Figure 14. This methodology is

ACCEPTED MANUSCRIPT

expected to be applicable to any type of volcaniclastic rock whatever their age. In many studies using geochronology on zircon grains extracted from volcaniclastic rocks, the obtained ages are often considered as sedimentation ages (e.g., Young, 2014, and references therein). The aforementioned examples illustrate some limitations on the interpretation of the obtained ages. Not only it is not straightforward to transform a date into an age (e.g., Spencer et al., 2016), but also the significance of an age obtained from detrital grains in volcaniclastic rocks requires careful evaluation. Indeed, any age obtained from volcaniclastic series should be considered, at first, as a maximum depositional age. In order to interpret this age as a sedimentation age, a series of maximum depositional ages must be acquired along the stratigraphic succession.

7. Conclusions

Because of their ubiquity in the sedimentary record and their propensity to bear datable minerals (e.g., zircon), volcaniclastic rocks have been extensively used to date deposition in sedimentary successions. However, to be valid and reliable, such dating must rely on the assumptions that (i) eruptions can be dated (i.e., from ages given by zircon autocrysts), and that (ii) volcanism and sedimentation were coeval. In ancient, weathered and/or poorly exposed volcaniclastic series, these assumptions are difficult to confirm, leading to potential misinterpretations of the obtained ages.

A relatively simple way to verify these assumptions consists in comparing series of maximum depositional ages with the stratigraphic position of the volcaniclastic beds combined with accurate sedimentological, mineralogical and geochemical analyses. When there is no maximum depositional ages getting younger upwards in a section, or when only a single age is available, it remains tricky to infer sedimentation ages without

ACCEPTED MANUSCRIPT

over-interpreting the available datasets. In contrast, when the maximum depositional ages get younger with sedimentation, volcanic activity and sedimentation were likely coeval. Such a result allows constraining the depositional ages of volcaniclastic rocks, whether they contain reworked volcaniclasts or not. Additionally, a time scale of reworking can be estimated.

Only two out of the five examples from this work show maximum depositional ages getting younger upwards in the section. However, from the literature, all these examples are assumed to represent cases of coeval volcanism and sedimentation. Even so, in the three other examples, this is impossible to prove from a strict geochronological point of view.

For two of the examples, the calculated time scales of reworking from the available data are less than 1 Myr and ca. 7 Myr, respectively. They likely relate the corresponding volcaniclastic layers to one or several eruptions from a single eruptive episode and to several eruptive episodes, respectively. These values are, however, dependent on both the available samples (from field and overall geological conditions for the selection of the dated minerals) and the analytical methods used in these studies.

The five examples illustrate that many factors, such as the occurrence or absence of autocrystic zircon grains, their relative abundance among zircon populations and their potential reworking, may influence the interpretation of geochronological results. These factors, which are often overlooked or ignored, should be taken into account in any geochronological study relying on volcano-sedimentary series to better assess the relevance of the obtained dates.

ACCEPTED MANUSCRIPT

Acknowledgements

Marie-Pierre Dabard, who dedicated part of her academic career to the study of volcaniclastic rocks, passed away too early, during the course of the elaboration of this manuscript. We dedicate this work to her memory. The geochronological analyses were supported by the Observatoire des Sciences de l'Univers de Rennes (OSUR). X. Le Coz, Y. Lepagnot (Géociences Rennes) and A. Lauqué are acknowledged for the thin sections, rock crushing and assistance for mineral separation, respectively. We are very grateful to J. Broutin (Université Pierre et Marie Curie, France), Shi Xiao (Jilin University, China), Zhang Wei and Chu Daoliang (China University of Geosciences, Wuhan, China) for their help and assistance during fieldwork, financially supported by the National Science Foundation of China (NSFC - programs 41272372 and 41572005). This work was supported by the FAPESP (Fundação Amparo à Pesquisa do Estado de São Paulo; processo 2018/02645-2 to C.R.). We acknowledge M. Nemeth, an anonymous reviewer and J. Knight for suggestions and comments that helped to clarify this manuscript.

References

Admakin, L.A., 2002. Accumulation and post-sedimentary diagenesis of tonsteins. Lithology and Mineral Resources 37, 60–67.

Allen, S.R., Hayward, B.W., Mathews, E., 2007. A facies model for a submarine volcaniclastic apron: The Miocene Manukau Subgroup, New Zealand. Bulletin of the Geological Society of America 119, 725–742.

Andersen, T., 2005. Detrital zircons as tracers of sedimentary provenance: limiting conditions from statistics and numerical simulation. Chemical Geology 216, 249–270.

ACCEPTED MANUSCRIPT

Bahlburg, H., Berndt, J., 2016. Provenance from zircon U-Pb age distributions in crustally contaminated granitoids. Sedimentary Geology 336, 161–170.

Baresel, B., D'Abzac, F.-X., Bucher, H., Schaltegger, U., 2016. High-precision time-space correlation through coupled apatite and zircon tephrochronology: An example from the Permian-Triassic boundary in South China. Geology 83, 83–86.

Bercovici, A., Bourquin, S., Broutin, J., Steyer, J.-S., Battail, B., Véran, M., Vacant, R., Khenthavong, B., Vongphamany, S., 2012. Permian continental paleoenvironments in Southeastern Asia: New insights from the Luang Prabang Basin (Laos). Journal of Asian Earth Sciences 60, 197–211.

Bernard, B., van Wyk de Vries, B., Leyrit, H., 2009. Distinguishing volcanic debris avalanche deposits from their reworked products: the Perrier sequence (French Massif Central). Bulletin of Volcanology 71, 1041–1056.

Best, M.G., Christiansen, E.H., 2001. Igneous petrology. Blackwell Science, Inc., Malden, USA, 458 pp.

Blanchard, S., Rossignol, C., Bourquin, S., Dabard, M.-P., Hallot, E., Nalpas, T., Poujol, M., Battail, B., Jalil, N.-E., Steyer, J.-S., Vacant, R., Véran, M., Bercovici, A., Diez, J.B., Paquette, J.-L., Khenthavong, B., Vongphamany, S., 2013. Late Triassic volcanic activity in South-East Asia: new stratigraphical, geochronological and paleontological evidence from the Luang Prabang Basin (Laos). Journal of Asian Earth Sciences 70-71, 8–26.

Bohor, B.F., Triplehorn, D.M., 1993. Tonsteins : altered volcanic-ash layers in coal-bearing sequences. The Geological Society of America, Inc., Boulder, Colorado, Special Paper 285, 44 pp.

Bourquin, S., Rossignol, C., Jolivet, M., Poujol, M., Broutin, J., Yu, J.-X., 2018a. Terrestrial Permian–Triassic boundary in southern China: New stratigraphic, structural and

ACCEPTED MANUSCRIPT

palaeoenvironment considerations. Palaeogeography, Palaeoclimatology, Palaeoecology 490, 640–652.

Bourquin, S., Rossignol, C., Jolivet, M., Poujol, M., Broutin, J., Yu, J., 2018b. Reply to the comment on "Terrestrial Permian-Triassic boundary in southern China: New stratigraphic, structural and palaeoenvironment considerations" by H. Zhang, Z. Feng, J. Ramezanik, S-Z Shen. Palaeogeography, Palaeoclimatology, Palaeoecology 506, 257-259.

Bull, S.W., Cas, R.A.F., 2000. Distinguishing base-surge deposits and volcaniclastic fluviatile sediments: an ancient example from the Lower Devonian Snowy River Volcanics, south-eastern Australia. Sedimentology 47, 87–98.

Burgess, S.D., Bowring, S.A., Shen, S.-Z., 2014. High-precision timeline for Earth's most severe extinction. Proceedings of the National Academy of Sciences 111, 3316–3321.

Burgess, S.D., Bowring, S.A., 2015. High-precision geochronology confirms voluminous magmatism before, during, and after Earth's most severe extinction. Science Advances 1, e1500470.

Busby, C., 2005. Possible distinguishing characteristics of very deepwater explosive and effusive silicic volcanism. Geology 33, 845–848.

Cassidy, M., Watt, S.F.L., Palmer, M.R., Trofimovs, J., Symons, W., Maclachlan, S.E., Stinton, A.J., 2014. Construction of volcanic records from marine sediment cores: A review and case study (Montserrat, West Indies). Earth-Science Reviews 138, 137–155.

Cawood, P.A., Hawkesworth, C.J., Dhuime, B., 2012. Detrital zircon record and tectonic setting. Geology 40, 875–878.

Charlier, B.L.A., Wilson, C.J.N., Lowenstern, J.B., Blake, S., van Calsteren, P.W., Davidson, J.P., 2005. Magma generation at a large, hyperactive silicic volcano (Taupo, New

ACCEPTED MANUSCRIPT

Zealand) revealed by U-Th and U-Pb systematics in zircons. Journal of Petrology 46, 3–32.

Charvet, J., Shu, L.S., Laurent-Charvet, S., Wang, B., Faure, M., Cluzel, D., Chen, Y., de Jong, K., 2011. Palaeozoic tectonic evolution of the Tianshan belt, NW China. Science China Earth Science 54, 166–184.

Chen, Z.-Q., Benton, M.J., 2012. The timing and pattern of biotic recovery following the end-Permian mass extinction. Nature Geoscience 5, 375–383.

Cherniak, D.J., Watson, E.B., 2001. Pb diffusion in zircon. Chemical Geology 172, 5–24.

Chew, D.M., Sylvester, P.J., Tubrett, M.N., 2011. U–Pb and Th–Pb dating of apatite by LA-ICPMS. Chemical Geology 280, 200–216.

Clayton, T., Francis, J.E., Hillier, S.J., Hodson, F., Saunders, R.A., Stone, J., 1996. The implications of reworking on the mineralogy and chemistry of lower Carboniferous K-bentonites. Clay Minerals 31, 377–390.

Cohen, K.M., Finney, S.C., Gibbard, P.L., Fan, J.-X., 2013 (updated, v2018/08). The ICS International Chronostratigraphic Chart. Episodes 36, 199-204.

Corfu, F., Hanchar, J.M., Hoskin, P.W.O., Kinny, P., 2003. Atlas of Zircon Textures. In: Hanchar, J.M., Hoskin, P.W.O. (Eds.), Zircon. Mineralogical Society of America and Geochemical Society, Washington, DC, United States, pp. 469–500.

Corfu, F., 2013. A century of U-Pb geochronology: The long quest towards concordance. Geological Society of America Bulletin 125, 33–47.

D'Atri, A., Dela Pierre, F., Lanza, R., Ruffmi, R., 1999. Distinguishing primary and resedimented vitric volcaniclastic layers in the Burdigalian carbonate shelf deposits in Monferrato (NW Italy). Sedimentary Geology 129, 143–163.

ACCEPTED MANUSCRIPT

Davidson, J.P., Morgan, D.J., Charlier, B.L.A., Harlou, R., Hora, J.M., 2007. Microsampling and Isotopic Analysis of Igneous Rocks: Implications for the Study of Magmatic Systems. Annual Review of Earth and Planetary Sciences 35, 273–311.

de Saint Blanquat, M., Horsman, E., Habert, G., Morgan, S., Vanderhaeghe, O., Law, R., Tikoff, B., 2011. Multiscale magmatic cyclicity, duration of pluton construction, and the paradoxical relationship between tectonism and plutonism in continental arcs. Tectonophysics 500, 20–33.

Deconinck, J.F., Crasquin, S., Bruneau, L., Pellenard, P., Baudin, F., Feng, Q., 2014. Diagenesis of clay minerals and K-bentonites in Late Permian/Early Triassic sediments of the Sichuan Basin (Chaotian section, Central China). Journal of Asian Earth Sciences 81, 28–37.

Denlinger, R.P., Hoblitt, R.P., 1999. Cyclic eruptive behavior of silicic volcanoes. Geology 27, 459–462.

Dickinson, W.R., Gehrels, G.E., 2009. Use of U–Pb ages of detrital zircons to infer maximum depositional ages of strata: A test against a Colorado Plateau Mesozoic database. Earth and Planetary Science Letters 288, 115–125.

Dodson, M.H., 1973. Closure temperature in cooling geochronological and petrological systems. Contributions to Mineralogy and Petrology 40, 259–274.

Eriksson, P.G., Catuneanu, O., Sarkar, S., Tirsgaard, H., 2005. Patterns of sedimentation in the Precambrian. Sedimentary Geology 176, 17–42.

Ernst, W.G., 2009. Archean plate tectonics, rise of Proterozoic supercontinentality and onset of regional, episodic stagnant-lid behavior. Gondwana Research 15, 243–253.

Fedo, C.M., Sircombe, K.N., Rainbird, R.H., 2003. Detrital Zircon Analysis of the Sedimentary Record. In: Hanchar, J.M., Hoskin, P.W.O. (Eds.), Zircon. Mineralogical

ACCEPTED MANUSCRIPT

Society of America and Geochemical Society, Washington, DC, United States, pp. 277–303.

Fisher, R.V., Schmincke, H.U., 1984. Pyroclastic rocks. Springer-Verlag Berlin, Heidelberg, 472 pp.

Fisher, R.V., Smith G.A., 1991. Volcanism, tectonics, and sedimentation. In: Fisher, R.V., Smith G.A. (Eds.), Sedimentation in tectonic settings. Society for Sedimentary Geology Special Publication 45, pp. 1-5.

Freundt, A., 2003. Entrance of hot pyroclastic flows into the sea: experimental observations. Bulletin of Volcanology 65, 144–164.

Galerne, C., Caroff, M., Rolet, J., Le Gall, B., 2006. Magma–sediment mingling in an Ordovician rift basin: The Plouézec–Plourivo half-graben, Armorican Massif, France. Journal of Volcanology and Geothermal Research 155, 164-178.

Gao, Q., Zhang, N., Xia, W., Feng, Q., Chen, Z.-Q., Zheng, J., Griffin, W.L., O'Reilly, S.Y., Pearson, N.J., Wang, G., Wu, S., Zhong, W., Sun, X., 2013. Origin of volcanic ash beds across the Permian–Triassic boundary, Daxiakou, South China: Petrology and U–Pb age, trace elements and Hf-isotope composition of zircon. Chemical Geology 360-361, 41–53.

Gastaldo, R.A., Kamo, S.L., Neveling, J., Geissman, J.W., Bamford, M., Looy, C.V., 2015. Is the vertebrate-defined Permian-Triassic boundary in the Karoo Basin, South Africa, the terrestrial expression of the end-Permian marine event? Geology 43, 939-942.

Gehrels, G.E., 2012. Detrital Zircon U-Pb Geochronology: Current Methods and New Opportunities. In: Busby, C., Perez, A.A. (Eds.), Recent Advances in Tectonics of Sedimentary Basins. Wiley, pp. 47–62.

Glorie, S., De Grave, J., Buslov, M.M., Elburg, M.A., Stockli, D.F., Gerdes, A., Van den haute, P., 2010. Multi-method chronometric constraints on the evolution of the Northern

ACCEPTED MANUSCRIPT

Kyrgyz Tien Shan granitoids (Central Asian Orogenic Belt): From emplacement to exhumation. Journal of Asian Earth Sciences 38, 131–146.

Gong, N., Hong, H., Huff, W.D., Fang, Q., Bae, C.J., Wang, C., Yin, K., Chen, S., 2018. Influences of Sedimentary Environments and Volcanic Sources on Diagenetic Alteration of Volcanic Tuffs in South China. Scientific Reports 8, doi:10.1038/s41598-018-26044-w

Harrison, T.M., Aleinikoff, J.N., Compston, W., 1987. Observations and controls on the occurrence of inherited zircon in Concord-type granitoids, New Hampshire. Geochimica et Cosmochimica Acta 51, 2549–2558.

He, B., Xu, Y.-G., Zhong, Y.-T., Guan, J.-P., 2010. The Guadalupian–Lopingian boundary mudstones at Chaotian (SW China) are clastic rocks rather than acidic tuffs: Implication for a temporal coincidence between the end-Guadalupian mass extinction and the Emeishan volcanism. Lithos 119, 10–19.

Heilbronn, G., 2014. Palaeogeographic and palaeotopographic evolution of the Chinese Tian Shan during the Mesozoic. Thèse, Université de Rennes 1, 267 pp.

Hendrix, M.S., 2000. Evolution of Mesozoic sandstone composition, southern Junggar, northern Tarim, and western Turpan basins, northwest China: a detrital record of the ancestral Tian Shan. Journal of Sedimentary Research 70, 520–532.

Hendrix, M., Graham, S.A., Carroll, A., Sobel, E., McKnight, C., Schulein, B., Wang, Z., 1992. Sedimentary record and climatic implications of recurrent deformation in the Tian Shan: Evidence from Mesozoic strata of the north Tarim, south Dzungar, and Turpan basin, northwest China. Geological Society of America Bulletin 104, 53-79.

Hildreth, W., Lanphere, M.A., 1994. Potassium-argon geochronology of a basalt-andesite-dacite arc system: the Mount Adams volcanic field, Cascade Range of southern Washington. Geological Society of America Bulletin 106, 1413–1429.

ACCEPTED MANUSCRIPT

Hong, H., Zhao, L., Fang, Q., Algeo, T.J., Wang, C., Yu, J., Gong, N., Yin, K., Ji, K., 2018. Volcanic sources and diagenetic alteration of Permian-Triassic boundary K-bentonites in Guizhou Province, South China. Palaeogeography. Palaeoclimatology. Palaeoecology, in press.

Honnorez, J., Kirst, P., 1975. Submarine basaltic volcanism: Morphometric parameters for discriminating hyaloclastites from hyalotuffs. Bulletin Volcanologique 39, 441–465.

Horstwood, M.S.A., Kosler, J., Gehrels, G., Jackson, S.E., McLean, N.M., Paton, C., Pearson, N.J., Sircombe, K., Sylvester, P., Vermeesch, P., Bowring, J.F., Condon, D.J., Schoene, B., 2016. Community-Derived Standards for LA-ICP-MS U-(Th-) Pb Geochronology – Uncertainty Propagation, Age Interpretation and Data Reporting. Geostandards Newsletter 40, 311–332.

Huff, W.D., 2016. K-bentonites: A review. American Mineralogist 101, 43–70.

Jackson, S.E., Pearson, N.J., Griffin, W.L., Belousova, E.A., 2004. The application of laser ablation-inductively coupled plasma-mass spectrometry to in situ U–Pb zircon geochronology. Chemical Geology 211, 47–69.

Jerram, D.A., Stollhofen, H., 2002. Lava-sediment interaction in desert settings; are all peperite-like textures the result of magma-water interaction? Journal of Volcanology and Geothermal Research 114, 231–249.

Jolivet, M., 2017. Mesozoic tectonic and topographic evolution of Central Asia and Tibet: a preliminary synthesis. In: Brunet, M.-F., McCann, T., Sobel, E.R. (Eds.), Geological evolution of the Central Asian basins and the western Tien Shan Range. Geological Society, London, Special Publication 427, pp. 19–55.

ACCEPTED MANUSCRIPT

Kataoka, K.S., Manville, V., Nakajo, T., Urabe, A., 2009. Impacts of explosive volcanism on distal alluvial sedimentation: Examples from the Pliocene–Holocene volcaniclastic successions of Japan. Sedimentary Geology 220, 306–317.

Kosler, J., Sylvester, P.J., 2003. Present Trends and the Future of Zircon in Geochronology: Laser Ablation ICPMS. In: Hanchar, J.M., Hoskin, P.W.O. (Eds.), Zircon. Mineralogical Society of America and Geochemical Society, pp. 243–275.

Lehrmann, D.J., Ramezani, J.A., Bowring, S.A., Martin, M.W., Montgomery, P., Enos, P., Payne, J.L., Orchard, M.J., Hongmei, W., Jiayong, W., 2006. Timing of recovery from the end-Permian extinction: Geochronologic and biostratigraphic constraints from south China. Geology 34, 1053–1056.

Le Maitre, R. W., Streckeisen, A., Zanettin, B., Le Bas, M. J., Bonin, B., Bateman, P., Bellieni, G., Dudek, A., Efremova, S., Keller, J., Lameyre, J., Sabine, P. A., Schmid, R., Sørensen, H., Woolley, A. R., 2002. Igneous rocks: A classification and glossary of terms (2nd ed), Cambridge University Press, United Kingdom 236 pp.

Lenhardt, N., Hornung, J., Hinderer, M., Böhnel, H., Torres-Alvarado, I.S., Trauth, N., 2011. Build-up and depositional dynamics of an arc front volcaniclastic complex: The Miocene Tepoztlán Formation (Transmexican Volcanic Belt, Central Mexico). Sedimentology 58, 785–823.

Lewis-Kenedi, C.B., Lange, R.A., Hall, C.M., Delgado-Granados, H., 2005. The eruptive history of the Tequila volcanic field, western Mexico: Ages, volumes, and relative proportions of lava types. Bulletin of Volcanology 67, 391–414.

Lexa, J., Seghedi, I., Németh, K., Szakács, A., Konečný, V., Pécskay, Z., Fülöp, A., Kovacs, M., 2010. Neogene-quaternary volcanic forms in the Carpathian-Pannonian region: A review, Central European Journal of Geosciences 2, 207-270.

ACCEPTED MANUSCRIPT

Li, S.-L., Tan, C.-P., Steel, R., Yu, X.H., 2014. Jurassic sedimentary evolution of southern Junggar Basin: Implication for palaeoclimate changes in northern Xinjiang Uygur Autonomous Region, China. Journal of Palaeogeography 3, 145–161.

Ludwig, K.R., 1998. On the Treatment of Concordant Uranium-Lead Ages. Geochimica et Cosmochimica Acta 62, 665–676.

Ludwig, K.R., 2012. User's Manual for a geochronological toolkit for Microsoft Excel. Berkeley Geochronological Center, 5, 75 pp.

Malusa, M.G., Carter, A., Limoncelli, M., Villa, I.M., Garzanti, E., 2013. Bias in detrital zircon geochronology and thermochronometry. Chemical Geology 359, 90–107.

Manville, V., Németh, K., Kano, K., 2009. Source to sink: A review of three decades of progress in the understanding of volcaniclastic processes, deposits, and hazards. Sedimentary Geology 220, 136–161.

Martin, U., Nemeth, K., 2007. Blocky versus fluidal peperite textures developed in volcanic conduits, vents and crater lakes of phreatomagmatic volcanoes in Mio/Pliocene volcanic fields of Western Hungary. Journal of Volcanology and Geothermal Research 159, 164–178.

Marzoli, A., Jourdan, F., Puffer, J.H., Cuppone, T., Tanner, L.H., Weems, R.E., Bertrand, H., Cirilli, S., Bellieni, G., De Min, A., 2011. Timing and duration of the Central Atlantic magmatic province in the Newark and Culpeper basins, eastern U.S.A. Lithos 122, 175–188.

Mattinson, J.M., 2005. Zircon U-Pb chemical abrasion ("CA-TIMS") method: Combined annealing and multi-step partial dissolution analysis for improved precision and accuracy of zircon ages. Chemical Geology 220, 47–66.

Mattioli, M., Lustrino, M., Ronca, S., Bianchini, G., 2012. Alpine subduction imprint in Apennine volcaniclastic rocks. Geochemical-petrographic constraints and

ACCEPTED MANUSCRIPT

geodynamic implications from Early Oligocene Aveto-Petrignacola Formation (N Italy). Lithos 134-135, 201–220.

Metcalfe, I., Crowley, J.L., Nicoll, R.S., Schmitz, M., 2015. High-precision U-Pb CA-TIMS calibration of Middle Permian to Lower Triassic sequences, mass extinction and extreme climate-change in eastern Australian Gondwana. Gondwana Research 28, 61–81.

Michaut, C., Ricard, Y., Bercovici, D., Sparks, R.S.J., 2013. Eruption cyclicity at silicic volcanoes potentially caused by magmatic gas waves. Nature Geoscience 6, 856–860.

Miller, J.S., Matzel, J.E.P., Miller, C.F., Burgess, S.D., Miller, R.B., 2007. Zircon growth and recycling during the assembly of large, composite arc plutons. Journal of Volcanology and Geothermal Research 167, 282–299.

Moorhouse, B.L., White, J.D.L., 2016. Interpreting ambiguous bedforms to distinguish subaerial base surge from subaqueous density - current deposits. The Depositional Record 2, 1–23.

Morton, A.C., Hallsworth, C.R., 1999. Processes controlling the composition of heavy mineral assemblages in sandstones. Sedimentary Geology 124, 3–29.

Nemchin, A.A., Cawood, P.A., 2005. Discordance of the U–Pb system in detrital zircons: Implication for provenance studies of sedimentary rocks. Sedimentary Geology 182, 143–162.

Orton, G.J., 1996. Volcanic environments. In: Reading, H.G. (Ed.), Sedimentary Environments: Processes, Facies and Stratigraphy. Blackwell Science, Oxford, pp. 485–567.

Ovtcharova, M., Bucher, H., Schaltegger, U., Galfetti, T., Brayard, A., Guex, J., 2006. New Early to Middle Triassic U–Pb ages from South China: Calibration with ammonoid

ACCEPTED MANUSCRIPT

biochronozones and implications for the timing of the Triassic biotic recovery. Earth and Planetary Science Letters 243, 463–475.

Pellenard, P., Deconinck, J.F., Huff, W.D., Thierry, J., Marchand, D., Fortwenglers, D., Trouiller, A., 2003. Characterization and correlation of Upper Jurassic (Oxfordian) bentonite deposits in the Paris Basin and the Subalpine Basin, France. Sedimentology 50, 1035–1060.

Pellenard, P., Gand, G., Schmitz, M., Galtier, J., Broutin, J., Stéyer, J.S., 2017. High-precision U-Pb zircon ages for explosive volcanism calibrating the NW European continental Autunian stratotype. Gondwana Research 51, 118–136.

Pidgeon, R.T., 1992. Recrystallisation of oscillatory zoned zircon: some geochronological and petrological implications. Contributions to Mineralogy and Petrology 110, 463–472.

Pullen, A., Ibanez-Mejia, M., Gehrels, G.E., Ibanez-Mejia, J.C., Pecha, M., 2014. What happens when n=1000? Creating large-n geochronological datasets with LA-ICP-MS for geologic investigations. Journal of Analytical Atomic Spectrometry 29, 971–980.

Ronov, A.B., 1972. Evolution of Rock Composition and Geochemical Processes in the Sedimentary Shell of the Earth. Sedimentology 19, 157–172.

Ross, P.S., Ukstins Peate, I., McClintock, M.K., Xu, Y.G., Skilling, I.P., White, J.D.L., Houghton, B.F., 2005. Mafic volcaniclastic deposits in flood basalt provinces: A review. Journal of Volcanology and Geothermal Research 145, 281–314.

Rossignol, C., Bourquin, S., Poujol, M., Hallot, E., Dabard, M.-P., Nalpas, T., 2016. The volcaniclastic series from the Luang Prabang Basin, Laos: A witness of a triassic magmatic arc ? Journal of Asian Earth Sciences 120, 159–183.

Roverato, M., Juliani, C., Dias-Fernandes, C.M., Capra, L., 2017. Paleoproterozoic andesitic volcanism in the southern Amazonian craton, the Sobreiro Formation: New insights

ACCEPTED MANUSCRIPT

from lithofacies analysis of the volcaniclastic sequences. Precambrian Research 289, 18–30.

Rubidge, B.S., Erwin, D.H., Ramezani, J., Bowring, S.A., de Klerk, W.J., 2013. High-precision temporal calibration of Late Permian vertebrate biostratigraphy: U-Pb zircon constraints from the Karoo Supergroup, South Africa. Geology 41, 363–366.

Saylor, J.E., Stockli, D.F., Horton, B.K., Nie, J., Mora, A., 2012. Discriminating rapid exhumation from syndepositional volcanism using detrital zircon double dating: Implications for the tectonic history of the Eastern Cordillera, Colombia. Geological Society of America Bulletin 124, 762–779.

Schaltegger, U., Schmitt, A.K., Horstwood, M.S.A., 2015. U-Th-Pb zircon geochronology by ID-TIMS, SIMS, and laser ablation ICP-MS: Recipes, interpretations, and opportunities. Chemical Geology 402, 89–110.

Schmid, R., 1981. Descriptive nomenclature and classification of pyroclastic deposits and fragments: Recommendations of the lUGS Subcommission on the Systematics of Igneous Rocks. Geology 9, 41–43.

Schoene, B., Condon, D.J., Morgan, L., McLean, N., 2013. Precision and accuracy in geochronology. Elements 9, 19–24.

Schoene, B., Samperton, K.M., Eddy, M.P., Keller, G., Adatte, T., Bowring, S.A., Khadri, S.F.R., Gertsch, B., 2015. U-Pb geochronology of the Deccan Traps and relation to the end-Cretaceous mass extinction. Science 347, 182–184.

Seltmann, R., Konopelko, D., Biske, G., Divaev, F., Sergeev, S., 2011. Hercynian post-collisional magmatism in the context of Paleozoic magmatic evolution of the Tien Shan orogenic belt. Journal of Asian Earth Sciences 42, 821–838.

Sheth, H.C., 2007. 'Large Igneous Provinces (LIPs)': Definition, recommended terminology, and a hierarchical classification. Earth-Science Reviews 85, 117–124.

ACCEPTED MANUSCRIPT

Shen, S.-Z., Crowley, J.L., Wang, Y., Bowring, S.A., Erwin, D.H., Sadler, P.M., Cao, C.-Q., Rothman, D.H., Henderson, C.M., Ramezani, J., Zhang, H., Shen, Y., Wang, X.-D., Wang, W., Mu, L., Li, W.-Z., Tang, Y.-G., Liu, X.-L., Liu, L.-J., Zeng, Y., Jiang, Y.-F., Jin, Y.-G., 2011. Calibrating the end-Permian mass extinction. Science 334, 1367–72.

Shipboard Scientific Party, 2001. Site 1184. In: Mahoney, J.J., Fitton, J.G., Wallace, P.J., et al., (Eds.), Proceedings of the Ocean Drilling Program. Initial Reports 92, [CD-ROM] 131 pp.

Slama, J., Kosler, J., Condon, D.J., Crowley, J.L., Gerdes, A., Hanchar, J.M., Horstwood, M.S.A., Morris, G.A., Nasdala, L., Norberg, N., Schaltegger, U., Schoene, B., Tubrett, M.N., Whitehouse, M.J., 2008. Plesovice zircon — A new natural reference material for U–Pb and Hf isotopic microanalysis. Chemical Geology 249, 1–35.

Slama, J., Kosler, J., 2012. Effects of sampling and mineral separation on accuracy of detrital zircon studies. Geochemistry Geophysics Geosystems 13, Q05007, doi:10.1029/2012GC004106

Sohn, Y.K., Park, K.H., Yoon, S.-H., 2008. Primary versus secondary and subaerial versus submarine hydrovolcanic deposits in the subsurface of Jeju Island, Korea. Sedimentology 55, 899–924.

Sohn, Y.K., Yoon, S.-H., 2010. Shallow-marine records of pyroclastic surges and fallouts over water in Jeju Island, Korea, and their stratigraphic implications. Geology 38, 763–766.

Sohn, Y.K., Ki, J.S., Jung, S., Kim, M.-C., Cho, H., Son, M., 2013. Synvolcanic and syntectonic sedimentation of the mixed volcaniclastic–epiclastic succession in the Miocene Janggi Basin, SE Korea. Sedimentary Geology 288, 40–59.

Spears, D.A., 2012. The origin of tonsteins, an overview, and links with seatearths, fireclays and fragmental clay rocks. International Journal of Coal Geology 94, 22–31.

ACCEPTED MANUSCRIPT

Spencer, C.J., Kirkland, C.L., Taylor, R.J.M., 2016. Strategies towards statistically robust interpretations of in situ U – Pb zircon geochronology. Geoscience Frontiers, 7, 581-589.

Stow, D.A.V., Taira, A., Ogawa, Y., Soh, W., 1998. Volcaniclastic sediments, process interaction and depositional setting of the Mio-Pliocene Miura Group, SE Japan. Sedimentary Geology 115, 351–381.

Tang, W., Zhang, Z., Li, J., Li, K., Chen, Y., Guo, Z., 2014. Late Paleozoic to Jurassic tectonic evolution of the Bogda area (northwest China): Evidence from detrital zircon U-Pb geochronology. Tectonophysics 626, 144–156.

Thomas, W.A., 2011. Detrital-zircon geochronology and sedimentary provenance. Lithosphere 3, 304–308.

Tiepolo, M., 2003. In situ Pb geochronology of zircon with laser ablation–inductively coupled plasma–sector field mass spectrometry. Chemical Geology 199, 159–177.

Turbeville, B.N., 1991. The influence of ephemeral processes on pyroclastic sedimentation in a rift-basin, volcaniclastic-alluvial sequence, Espanola basin, New Mexico. Sedimentary Geology 74, 139–155.

Turner, S., Costa, F., 2007. Measuring timescales of magmatic evolution. Elements 3, 267–272.

Twitchett, R.J., Looy, C.V., Morante, R., Visscher, H., Wignall, P.B., 2001. Rapid and synchronous collapse of marine and terrestrial ecosystems during the end-Permian biotic crisis. Geology 29, 351-354.

Ver Straeten, C.A., 2004. K-bentonites, volcanic ash preservation, and implications for Early to Middle Devonian volcanism in the Acadian orogen, eastern North America. Bulletin of the Geological Society of America 116, 474–489.

ACCEPTED MANUSCRIPT

Vermeesch, P., 2004. How many grains are needed for a provenance study? Earth and Planetery Science Letters 224, 441–451.

Vermeesch, P., 2012. On the visualisation of detrital age distributions. Chemical Geology 312–313, 190–194.

Voight, B., Hoblitt, R.P., Clarke, A.B., Lockhart, A.B., Miller, A.D., Lynch, L., McMahon, J., 1998. Remarkable cyclic ground deformation monitored in real-time on Montserrat, and its use in eruption forecasting. Geophysical Research Letters 25, 3405–3408.

von Eynatten, H., Dunkl, I., 2012. Assessing the sediment factory: The role of single grain analysis. Earth-Science Reviews 115, 97–120.

Waitt, R.B., 2007. Primary volcaniclastic rocks: Comment and Reply: Comment. Geology 35, e141–e141.

Wang, J., Shao, L.-Y., Wang, H., Spiro, B., Large, D., 2018. SHRIMP zircon U–Pb ages from coal beds across the Permian–Triassic boundary, eastern Yunnan, southwestern China. Journal of Palaeogeography 7, 117–129.

White, J.D.L., Houghton, B.F., 2006. Primary volcaniclastic rocks. Geology 34, 677–680.

Wiedenbeck M., Alle P., Corfu F, Griffin W.L., Meier M., Oberli F., von Quadt A., Roddick J.C., Spiegel W., 1995. Three natural zircon standards for U-Th-Pb, Lu-Hf, trace element and REE analyses. Geostandards Newsletter 19, 1–23.

Wotzlaw, J.F., Hüsing, S.K., Hilgen, F.J., Schaltegger, U., 2014. High-precision zircon U-Pb geochronology of astronomically dated volcanic ash beds from the Mediterranean Miocene. Earth and Planetary Science Letters 407, 19–34.

Wray, D.S., Wood, C.J., 1998. Distinction between detrital and volcanogenic clay-rich beds in Turonian-Coniacian chalks of eastern England. Proceedings of the Yorkshire Geological Society 52, 95–105.

ACCEPTED MANUSCRIPT

Xie, X., Heller, P.L., 2009. Plate tectonics and basin subsidence history. Geological Society of America Bulletin 121, 55–64.

Yakymchuk, C., Brown, M., 2014. Behaviour of zircon and monazite during crustal melting. Journal of the Geological Society of London 171, 465–479.

Yang, J., Cawood, P.A., Du, Y., Huang, H., Tao, P., 2012. Large Igneous Province and magmatic arc sourced Permian–Triassic volcanogenic sediments in China. Sedimentary Geology 261-262, 120–131.

Yang, W., Jolivet, M., Dupont-Nivet, G., Guo, Z., Zhang, Z., Wu, C., 2013. Source to sink relations between the Tian Shan and Junggar Basin (northwest China) from Late Palaeozoic to Quaternary: Evidence from detrital U-Pb zircon geochronology. Basin Research 25, 219–240.

Young, G.M., 2014. Contradictory correlations of Paleoproterozoic glacial deposits: Local, regional or global controls? Precambrian Research 247, 33–44.

Yu, J., Peng, Y., Zhang, S., Yang, F., Zhao, Q., Huang, Q., 2007. Terrestrial events across the Permian–Triassic boundary along the Yunnan–Guizhou border, SW China. Global and Planetary Change 55, 193–208.

Yu, J., Li, H.M., Zhang, S.X., Yang, F.Q., Feng, Q.L., 2008. Timing of the terrestrial Permian-Triassic boundary biotic crisis: Implications from U-Pb dating of authigenic zircons. Science in China Series D: Earth Sciences 51, 1633–1645.

Yu, J., Broutin, J., Chen, Z.Q., Shi, X., Li, H., Chu, D., Huang, Q., 2015. Vegetation changeover across the Permian-Triassic Boundary in Southwest China. Extinction, survival, recovery and palaeoclimate: A critical review. Earth-Science Reviews 149, 203–224.

Zakharov, D.O., Bindeman, I.N., Slabunov, A., Ovtcharova, M., Coble, M.A., Serebryakov, N.S., Schaltegger, U., 2017. Dating the Paleoproterozoic snowball Earth glaciations using contemporaneous subglacial hydrothermal systems. Geology 45, 667–670.

ACCEPTED MANUSCRIPT

Zhang, H., Cao, C.-Q., Liu, X.-L., Mu, L., Zheng, Q.-F., Liu, F., Xiang, L., Liu, L.-J., Shen, S.-Z., 2016. The terrestrial end-Permian mass extinction in South China. Palaeogeography, Palaeoclimatology, Palaeoecology 448, 108–124.

Zhang, X., Zhao, G., Sun, M., Eizenhöfer, P.R., Han, Y., Hou, W., Liu, D., Wang, B., Liu, Q., Xu, B., 2016. Tectonic evolution from subduction to arc-continent collision of the Junggar ocean: Constraints from U-Pb dating and Hf isotopes of detrital zircons from the North Tianshan belt, NW China. Bulletin of the Geological Society of America 128, 644–660.

Zhang, H., Feng, Z., Ramezani, J., Shen, S.-Z., 2018. Comments on "Terrestrial Permian–Triassic boundary in southern China: New stratigraphic, structural and palaeoenvironment considerations" by Bourquin et al. (2018). Palaeogeography, Palaeoclimatology, Palaeoecology 506, 254-256.

Zhu, S., Yue, H., Zhu, X., Sun, S., Wei, W., Liu, X., Jia, Y., 2017. Dolomitization of felsic volcaniclastic rocks in continental strata: A study from the Lower Cretaceous of the A'nan Sag in Er'lian Basin, China. Sedimentary Geology 353, 13–27.

Zimmermann, S., Mark, C., Chew, D., Voice, P.J., 2018. Maximising data and precision from detrital zircon U-Pb analysis by LA-ICPMS: The use of core-rim ages and the single-analysis concordia age. Sedimentary Geology 375, 5-13.

Figures and tables caption

Figures

Fig. 1. Basic classification scheme for volcaniclastic rocks.

ACCEPTED MANUSCRIPT

Fig. 2. Detections limits for one and three grains at the 50% and 95% confidence levels.

Fig. 3. Diagrams represent schematic stratigraphic log indicating relative sedimentation ages *versus* absolute time scale. (A) Maximum depositional ages getting younger upwards in the section: maximum depositional ages provide estimates of the actual depositional ages of the pile. (B) Maximum depositional ages getting older upwards in the section: volcanic activity and sedimentation were diachronous. (C) Overlapping uncertainties on the obtained maximum depositional ages along the pile: not possible to infer if volcanism and sedimentation were coeval (D) Maximum depositional ages uncorrelated with the sedimentation ages: maximum depositional ages likely derived from zircon populations that are not autocrystic in origin (i.e., antecryst, xenocryst, inherited and/or epiclastic populations).

Fig. 4. Characterizing how coeval volcanism and sedimentation are using the reworking time scale. (A) Schematic representation of the reworking time scale (Δt). T_{sed}: sedimentation age; T_{volc}: eruption age; T_{max}: maximum depositional age, depicted with a hypothetical analytical uncertainty (horizontal bar). (B) Formal definition of the reworking time scale, with end-member values.

Fig. 5. Duration of reworking (Δt): theoretical and practical considerations. Legend: same as in Fig. 4. $\Delta t_{theoretical}$, as defined Fig. 4. In practice, Tsed is *a priori* unknown, and only $\Delta t_{practical}$ can be estimated using 2 maximum depositional ages (and their uncertainties) that do not overlap, from 2 successive samples in a volcaniclastic series with absolute ages getting younger upwards.

ACCEPTED MANUSCRIPT

Fig. 6. Possible interpretations of overlapping maximum depositional ages. Legend: same as in Fig. 4. The cases A, B and C cannot be distinguished from geochronological datasets only. (A) Uncertainties larger than the reworking time scales for the successive volcaniclastic layers, assuming the maximum depositional ages are from zircon autocrysts. (B) Maximum depositional ages calculated from zircon autocrysts from the "Volc v" eruption and from zircon antecrysts from the "Volc v+1" eruption. Autocrysts and antecrysts crystallized at the same time, during the same magmatic stage. (C) Volcanic deposits produced during the oldest eruption (Volc v) less erodible than those produced during the youngest eruption (Volc v+1): volcaniclasts associated with the "Volc v" eruption deposited in the sedimentary layer "s+1", while those relating to the "Volc v+1" eruption eventually deposited earlier, in the sedimentary layer "s".

Fig. 7. Location, depositional environments and analytical techniques of the selected examples. Modified after Jolivet (2015), with main active faults and main Cenozoic basins (beige).

Fig. 8. Example of a sedimentary succession containing volcaniclastic layers with reworked volcaniclasts.

Fig. 9. Example of a sedimentary succession containing three volcaniclastic layers where the reworking time scale(s) cannot be constrained.

Fig. 10. Example of a sedimentary sequence containing volcaniclastic layers characterized by relatively short (< 1.5 Myr) reworking times.

ACCEPTED MANUSCRIPT

Fig. 11. Example of volcaniclastic rocks made up of reworked volcaniclasts displaying relatively long (<7.5 Myr) reworking times.

Fig. 12. Example of a volcanic rock devoid of zircon autocryst. (A) Hand specimen of the analyzed volcanic tuff collected in the Wusu Section (located in Fig. 7). Plant fragments are fossilized within the volcanic ash deposits. (B) Age distribution obtained from zircon grains extracted in a Middle Jurassic tuff of the Wusu Section. The age probability distribution was estimated using a bandwidth of 6.6 with Density Plotter 8.2 (Vermeesch, 2012) from all concordant dates (N=35).

Fig. 13. Possible correspondences between the cycles of volcanic activities; duration of the reworking times and resulting volcaniclastic rock units. Hierarchies of the time units and their durations are from Manville et al. (2009). (A) Volcaniclastic rocks units resulting from the reworking of the products of a single eruption ("eruption unit"). (B) Tephra units, generally made of mixed products from several eruptions and corresponding to longer reworking time scale. (C) Volcaniclastic deriving from the erosion, mixing and deposition of the products of several eruptions, possibly from several distinct volcanoes, likely corresponding to longer reworking time scale. (D) Erosion and sedimentation of products of various volcanoes belonging to a volcanic province corresponding to the longest reworking time scales. (E) Erosion of an old volcanic basement producing volcaniclastic rocks unrelated to volcanic activity.

Fig. 14. General methodology for the geochronological interpretation of volcaniclastic deposits.

ACCEPTED MANUSCRIPT

Tables

Table 1. Terminology for consolidated volcaniclastic rocks.

Table 2. Analytical methods, detection limits and maximum depositional ages of the samples.

Appendices

Appendix A. Detection limits for one and three grains at the 50% and 95% confidence levels.

Appendix B. Compilation of the U-Pb dating on zircon used to provide examples and details on the calculation of maximal depositional ages. Data sources: Gao et al. (2013); Lehrmann et al. (2006); Yu et al. (2008); Shen et al. (2011); Blanchard et al. (2013) and Rossignol et al. (2016).

Appendix C. Analytical DRX results for the claystone beds of the Chahe Section, Guizhou, south China

Appendix D. Analytical methods, data filtering and maximum depositional age calculation for complementary U-Pb geochronology on zircon grains.

Appendix E. Analytical results for complementary U-Pb geochronology on zircon grains.

ACCEPTED MANUSCRIPT

Table 1. Terminology for consolidated volcaniclastic rocks.

Average clast size	Pyroclastic	Tuffites	Epiclastic
d > 64 mm	Agglomerate, pyroclastic breccia	Tuffaceous conglomerate	Conglomerate
2 mm < d ≤ 64 mm	Lapillistone		
62 µm < d ≤ 2 mm	Coarse tuff	Tuffaceous sandstone	Sandstone
4 µm < d ≤ 62 µm	Fine tuff	Tuffaceous siltstone	Siltstone
d ≤ 4 µm		Tuffaceous mudstone	Mudstone
Volcaniclast content (vol.)	≥ 75% if pyroclasts	> 25%	≤ 25%

d: average grain size.
Modified after Le Maitre et al. (2002) and Schmid (1981).

ACCEPTED MANUSCRIPT

ACCEPTED MANUSCRIPT

Table 2. Analytical methods, detection limits and maximum depositional ages of the samples for the selected examples.

Sample[1]	Probability of concordance ≥ 10%, decay constants errors included									
	N	Detection limits[2] (%)				Maximum depositional age				
		$DL_{1(pL=0.5)}$	$DL_{1(pL=0.95)}$	$DL_{3(pL=0.5)}$	$DL_{3(pL=0.95)}$	concordia age	± 2σ	n	MSWD	Probability
Daxiakou Section – Analytical method: LA-ICP-MS										Gao et al., 2013
b.277	18	3.8	15.3	14.6	31.1	249.7	1.7	15	0.95	0.54
b.271	16	4.2	17.1	16.4	34.4	249.4	1.9	14	1.2	0.21
b.266	20	3.4	13.9	13.2	28.3	251.7	1.7	14	1.3	0.11
b.264	18	3.8	15.3	14.6	31.1	253.0	1.6	13	1.2	0.20
b.260	31	2.2	9.2	8.6	19.0	249.7	1.4	22	0.95	0.56
b.259-b	30	2.3	9.5	8.9	19.6	250.1	1.4	23	0.92	0.62
b.258	26	2.6	10.9	10.2	22.3	250.0	1.8	15	1.17	0.24
b.255	19	3.6	14.6	13.9	29.6	250.0	1.8	11	1.19	0.25
b.252	13	5.2	20.6	20.1	41.1	248.8	1.8	11	0.73	0.81
b.249	10	6.7	25.9	25.9	50.7	246.8	2.0	9	1.3	0.21
Chahe Section – Analytical methods: CA-TIMS (sample ch68; Shen et al., 2011), classical ID-TIMS (samples b.68a and b.68c; Yu et al., 2008) and LA-ICP-MS (samples CH63 and CH68, Appendices D and E)										
b.68c	4	15.9	52.7	61.5	90.3	247.5	3.0	3	0.09	0.99
b.68a	5	12.9	45.1	50.0	81.1	252.6	2.7	5	0.09	1.00
CH 68	36	1.9	8.0	7.4	16.5	252.4	1.5	20	0.44	1.00
ch68	8	8.3	31.2	32.1	60.0	252.35	0.23	5	1.8	0.06
CH 63	10	6.7	25.9	25.9	50.7	251.0	1.9	11	0.90	0.60
Guandao Section – Analytical methods: Air abraded and CA-TIMS										Lehrmann et al., 2006
tuff 110	16	4.2	17.1	16.4	34.4	245.97	0.28	8	1.4	0.14
tuff 3	15	4.5	18.1	17.5	36.4	246.82	0.23	5	1.9	0.05
tuff 2	16	4.2	17.1	16.4	34.4	247.38	0.22	11	0.55	0.95
tuff 1	15	4.5	18.1	17.5	36.4	247.26	0.22	9	1.5	0.30
Luang Prabang Basin – Analytical method: LA-ICP-MS										Blanchard et al., 2013; Rossignol et al., 2016
LP 45	14	4.8	19.3	18.7	38.6	215.9	1.3	15	0.66	0.92
LP 44	25	2.7	11.3	10.6	23.2	218.9	1.6	10	0.41	0.99
LP 100	40	1.7	7.2	6.7	15.0	220.9	1.1	27	0.62	0.99
LP 58	24	2.8	11.7	11.0	24.0	224.1	2.8	4	0.41	0.90
LP 57	27	2.5	10.5	9.8	21.6	225.0	1.3	17	0.58	0.97
Wusu Section – Analytical method: LA-ICP-MS										Appendices D and E
WU 01	35	2.0	8.2	7.6	17.0	n.a.				

1: for each section, the samples are presented following the stratigraphic order (the oldest to the bottom, the youngest to the top).
2: a detection limit is defined as the relative abundance of the largest population of zircon grains likely to remain undetected by a given number of analyzed grains – N in the present case (Andersen, 2005). See Appendix A.
LA-ICP-MS: Laser Ablation – Inductively Coupled Plasma – Mass Spectrometry. Typical analytical precision: ca. 1%.
CA-TIMS: Chemically Abraded – Thermal Ionization Mass Spectrometry. Air abraded method: similarly to the chemical abrasion of zircon grains, a mechanical ("air") abrasion can be used. Typical analytical precision: ca. 0.1%.
Typical analytical precision of classical Isotopic Dilution - TIMS method: ca. 1%.
N: total number of concordant zircon grains, generally corresponding to the number of analyses, except when more than one analysis per grain has been performed (e.g., sample CH 63); n: number of analyses used to calculate the maximum deposition age; DL_1: detection limit for at least 1 grain; DL_3: detection limit for at least 3 grains; $_{pL}$: probability level assigned to the detection limits; MSWD: mean square of weighted deviates. The MSWD and the probability given for the concordia ages are for both concordance and equivalence.

ACCEPTED MANUSCRIPT

ACCEPTED MANUSCRIPT

ACCEPTED MANUSCRIPT

Highlights

- Volcaniclastic rocks are extensively used to constrain sedimentation ages
- Dating a deposition requires the following two conditions
- If any, the autocryst minerals provided by the latest eruption must yield an age
- Volcanism and sedimentation must, in addition, have been coeval
- Reworking time-scale provides clues to discuss links between volcanoes and basins

ACCEPTED MANUSCRIPT

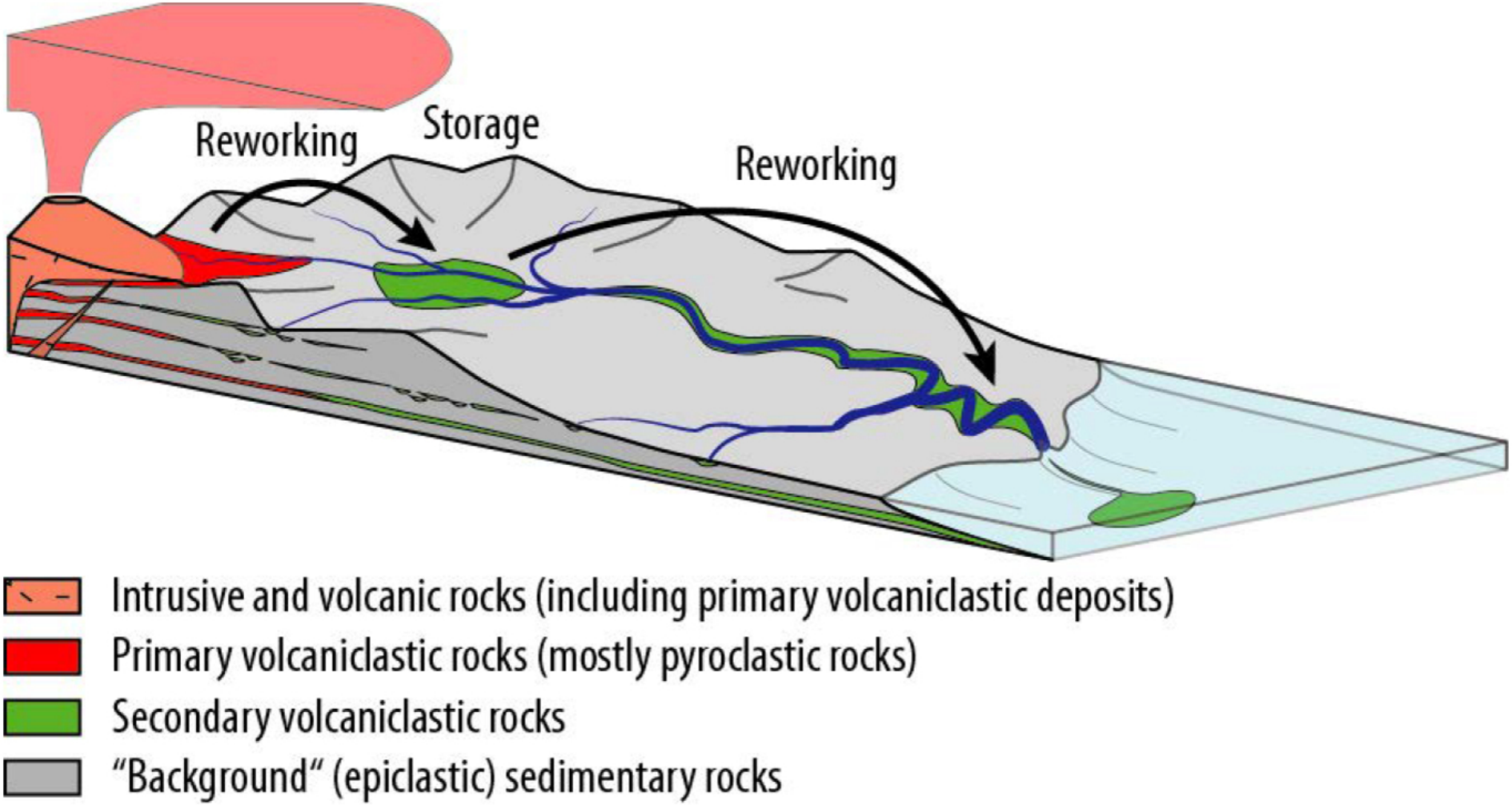

Reworking
Storage
Reworking
Intrusive and volcanic rocks (including primary volcaniclastic deposits)
Primary volcaniclastic rocks (mostly pyroclastic rocks)
Secondary volcaniclastic rocks
"Background" (epiclastic) sedimentary rocks

Figure 1

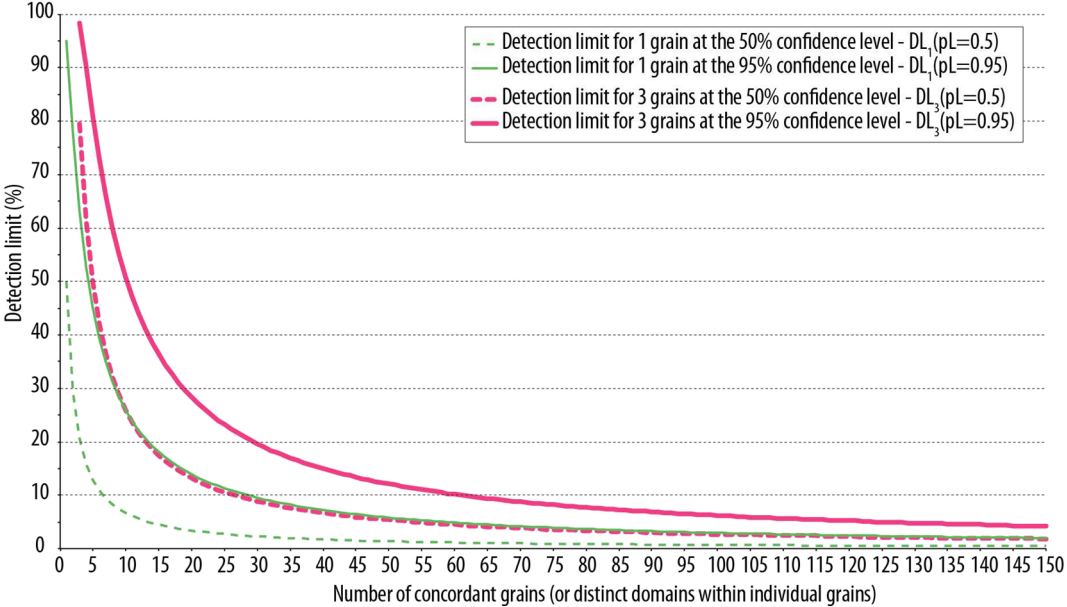

Detection limit for 1 grain at the 50% confidence level - DL1(pL=0.5)
Detection limit for 1 grain at the 95% confidence level - DL1(pL=0.95)
Detection limit for 3 grains at the 50% confidence level - DL3(pL=0.5)
Detection limit for 3 grains at the 95% confidence level - DL3(pL=0.95)
Detection limit (%)
100
90
80
70
60
50
40
30
20
10
0
0 5 10 15 20 25 30 35 40 45 50 55 60 65 70 75 80 85 90 95 100 105 110 115 120 125 130 135 140 145 150
Number of concordant grains (or distinct domains within individual grains)

Figure 2

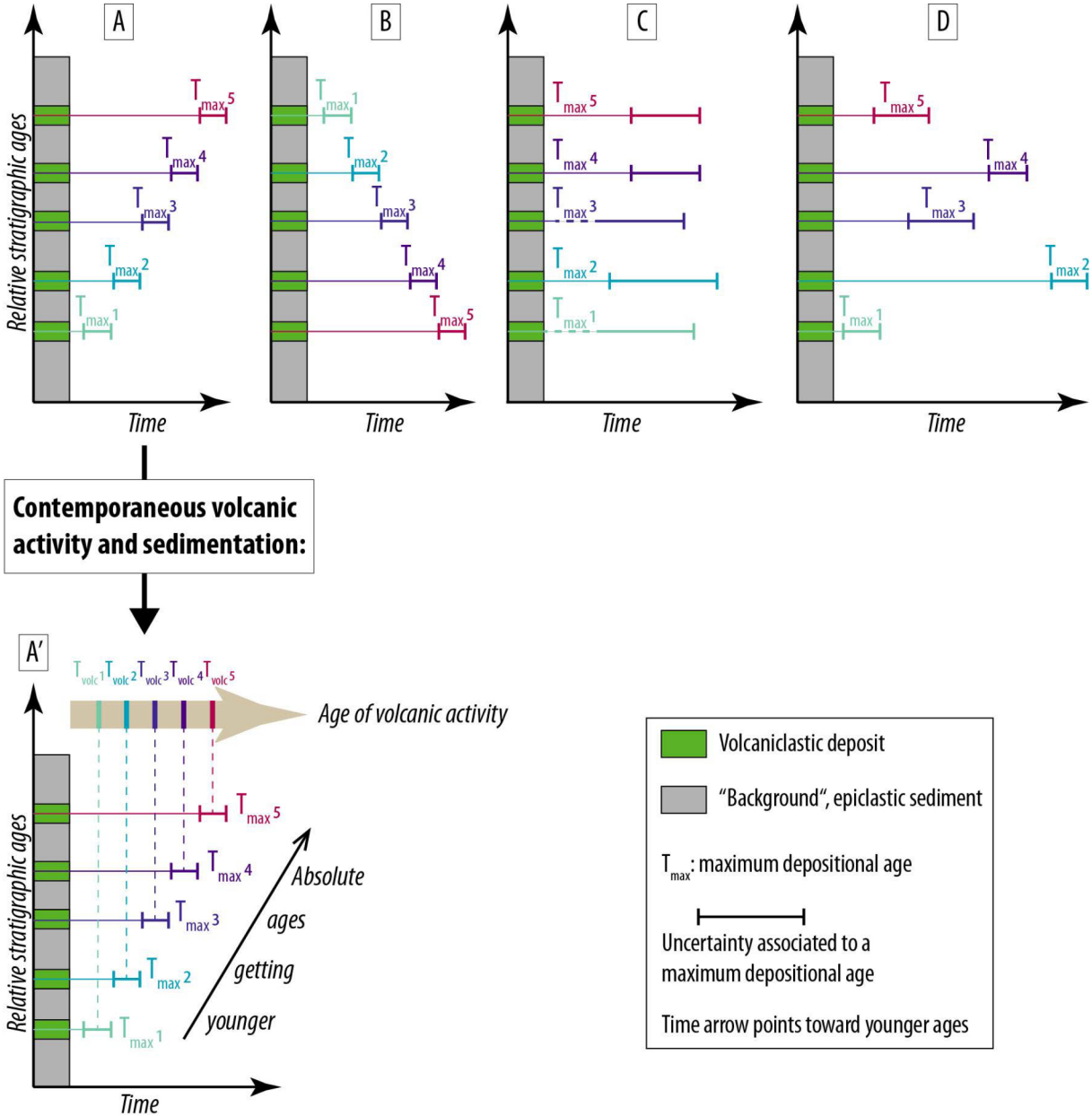

A
B
C
D
Relative stratigraphic ages
Time
Contemporaneous volcanic activity and sedimentation:
A′
Age of volcanic activity
Absolute ages getting younger
Volcaniclastic deposit
"Background", epiclastic sediment
T max: maximum depositional age
Uncertainty associated to a maximum depositional age
Time arrow points toward younger ages

Figure 3

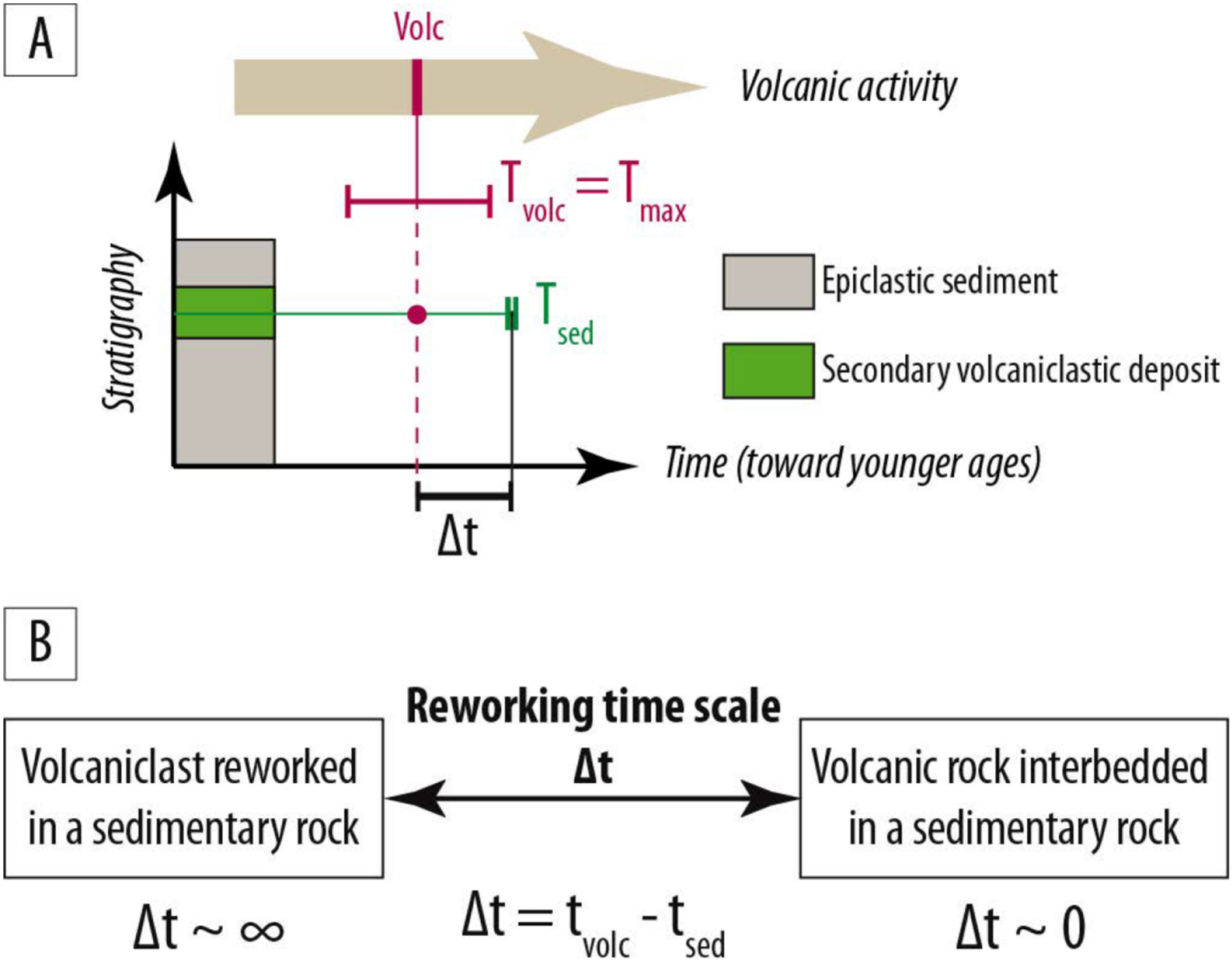

A
Volc
Volcanic activity
$T_{volc} = T_{max}$
T_{sed}
Stratigraphy
Epiclastic sediment
Secondary volcaniclastic deposit
Time (toward younger ages)
Δt
B
Reworking time scale
Δt
Volcaniclast reworked in a sedimentary rock
Volcanic rock interbedded in a sedimentary rock
Δt ~ ∞
$\Delta t = t_{volc} - t_{sed}$
Δt ~ 0

Figure 4

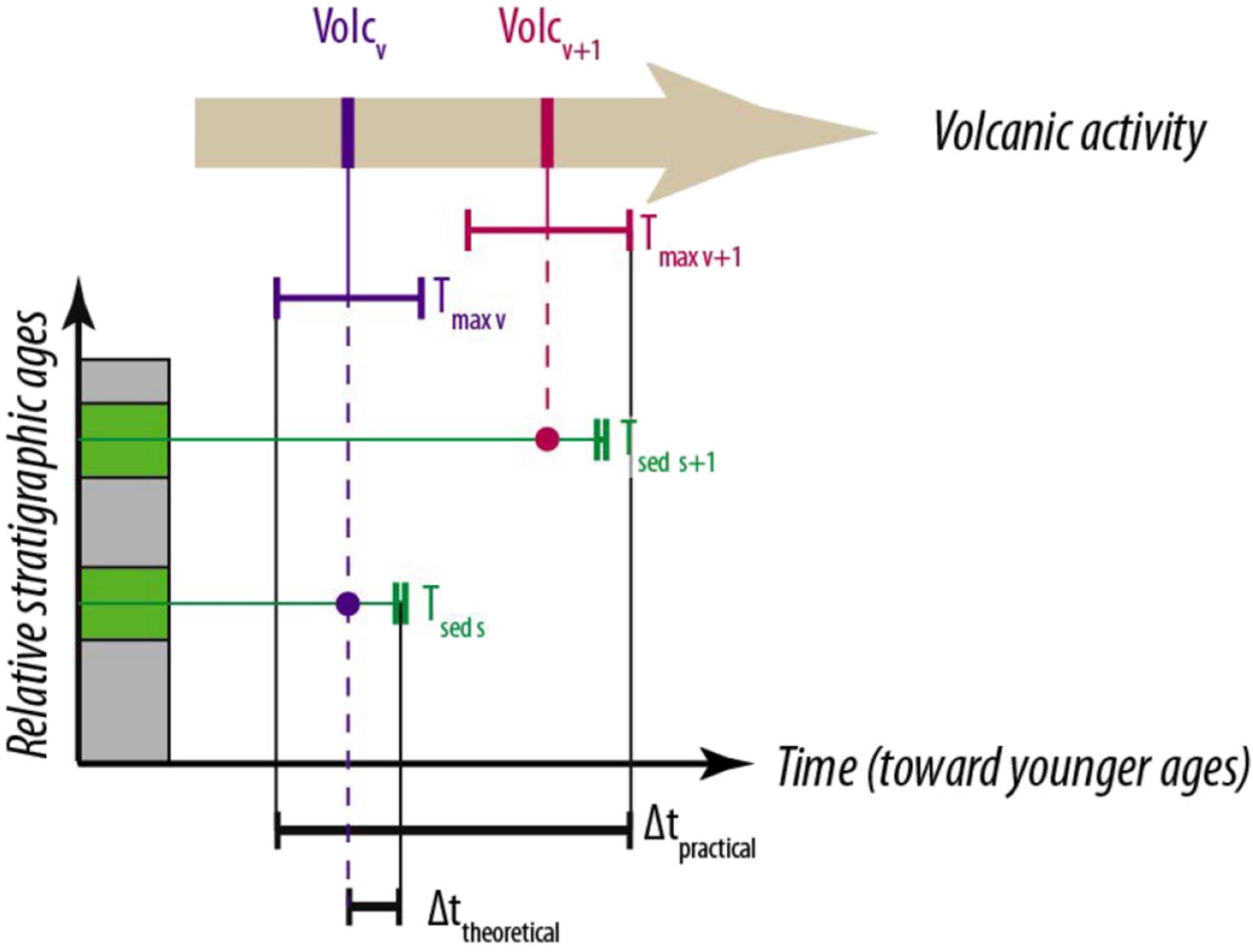

Volc v
Volc v+1
Volcanic activity
T max v+1
T max v
T sed s+1
T sed s
Relative stratigraphic ages
Time (toward younger ages)
Δt practical
Δt theoretical

Figure 5

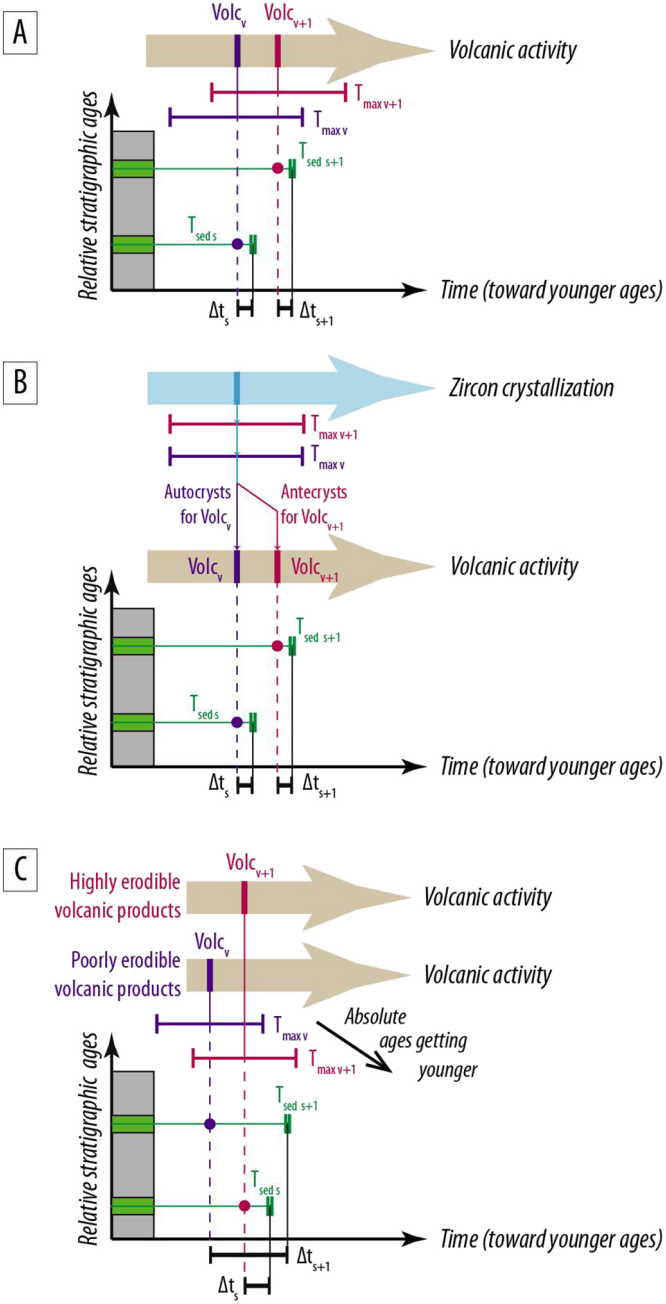

A
Volc$_v$
Volc$_{v+1}$
Volcanic activity
T$_{max\ v+1}$
T$_{max\ v}$
T$_{sed\ s+1}$
T$_{sed\ s}$
Relative stratigraphic ages
Time (toward younger ages)
Δt$_s$
Δt$_{s+1}$
B
Zircon crystallization
T$_{max\ v+1}$
T$_{max\ v}$
Autocrysts for Volc$_v$
Antecrysts for Volc$_{v+1}$
Volc$_v$
Volc$_{v+1}$
Volcanic activity
T$_{sed\ s+1}$
T$_{sed\ s}$
Relative stratigraphic ages
Time (toward younger ages)
Δt$_s$
Δt$_{s+1}$
C
Volc$_{v+1}$
Highly erodible volcanic products
Volcanic activity
Volc$_v$
Poorly erodible volcanic products
Volcanic activity
T$_{max\ v}$
T$_{max\ v+1}$
Absolute ages getting younger
T$_{sed\ s+1}$
T$_{sed\ s}$
Relative stratigraphic ages
Time (toward younger ages)
Δt$_{s+1}$
Δt$_s$

Figure 6

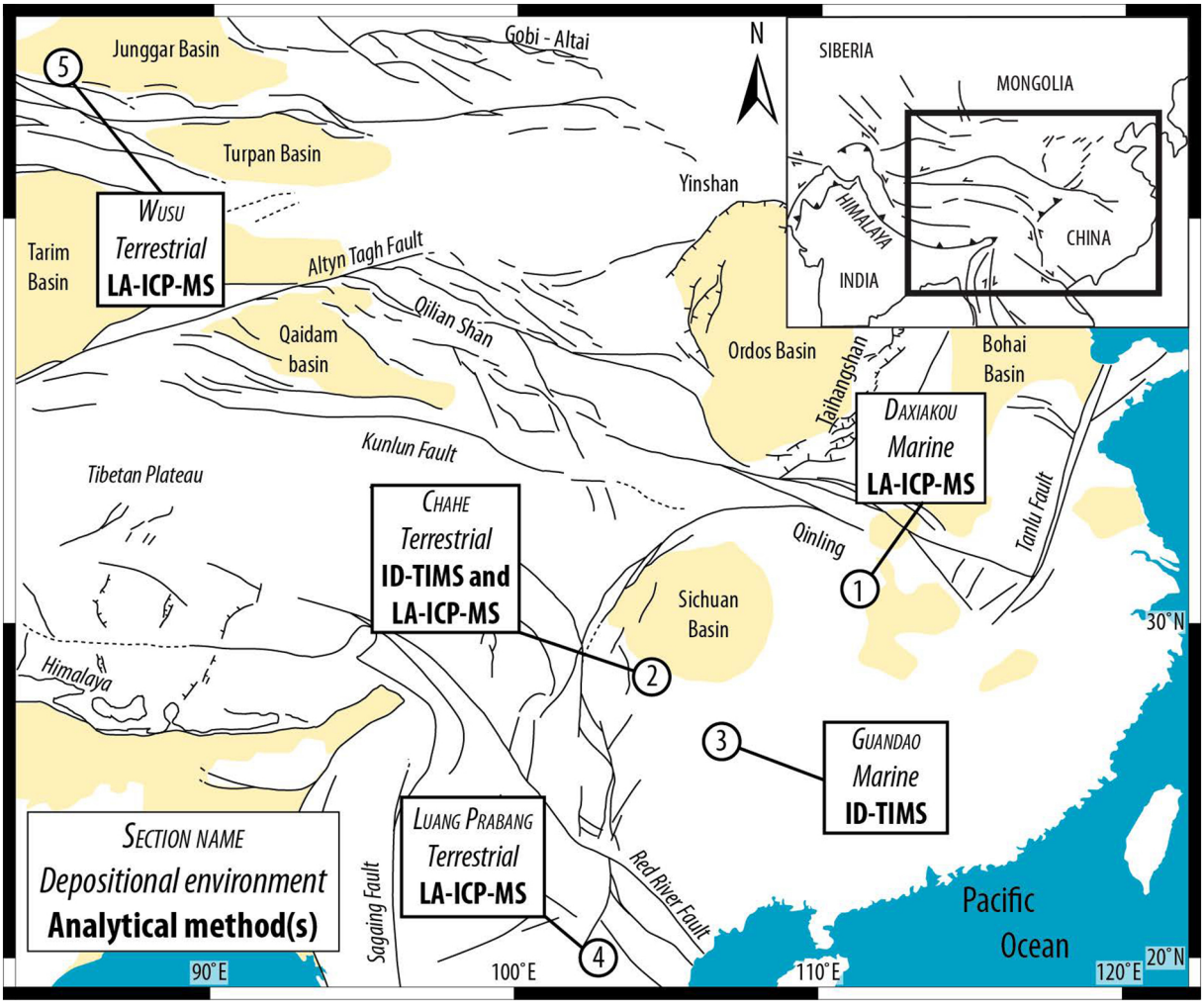

Junggar Basin
Gobi - Altai
N
SIBERIA
MONGOLIA
5
Turpan Basin
Yinshan
HIMALAYA
CHINA
INDIA
WUSU
Terrestrial
LA-ICP-MS
Tarim
Basin
Altyn Tagh Fault
Qilian Shan
Qaidam
basin
Ordos Basin
Taihangshan
Bohai
Basin
DAXIAKOU
Marine
LA-ICP-MS
Kunlun Fault
Tibetan Plateau
CHAHE
Terrestrial
ID-TIMS and
LA-ICP-MS
Qinling
Tanlu Fault
1
Sichuan
Basin
30°N
Himalaya
2
3
GUANDAO
Marine
ID-TIMS
SECTION NAME
Depositional environment
Analytical method(s)
LUANG PRABANG
Terrestrial
LA-ICP-MS
Red River Fault
Sagaing Fault
4
Pacific
Ocean
90°E
100°E
110°E
120°E
20°N

Figure 7

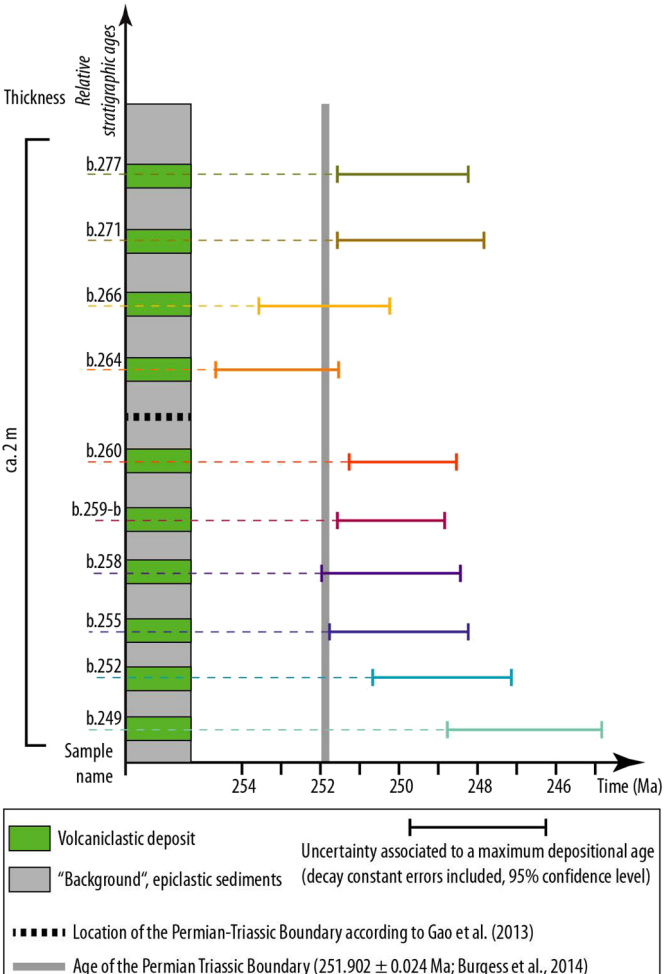

Thickness
Relative stratigraphic ages
ca. 2 m
b.277
b.271
b.266
b.264
b.260
b.259-b
b.258
b.255
b.252
b.249
Sample name
254
252
250
248
246
Time (Ma)
Volcaniclastic deposit
"Background", epiclastic sediments
Uncertainty associated to a maximum depositional age (decay constant errors included, 95% confidence level)
Location of the Permian-Triassic Boundary according to Gao et al. (2013)
Age of the Permian Triassic Boundary (251.902 ± 0.024 Ma; Burgess et al., 2014)

Figure 8

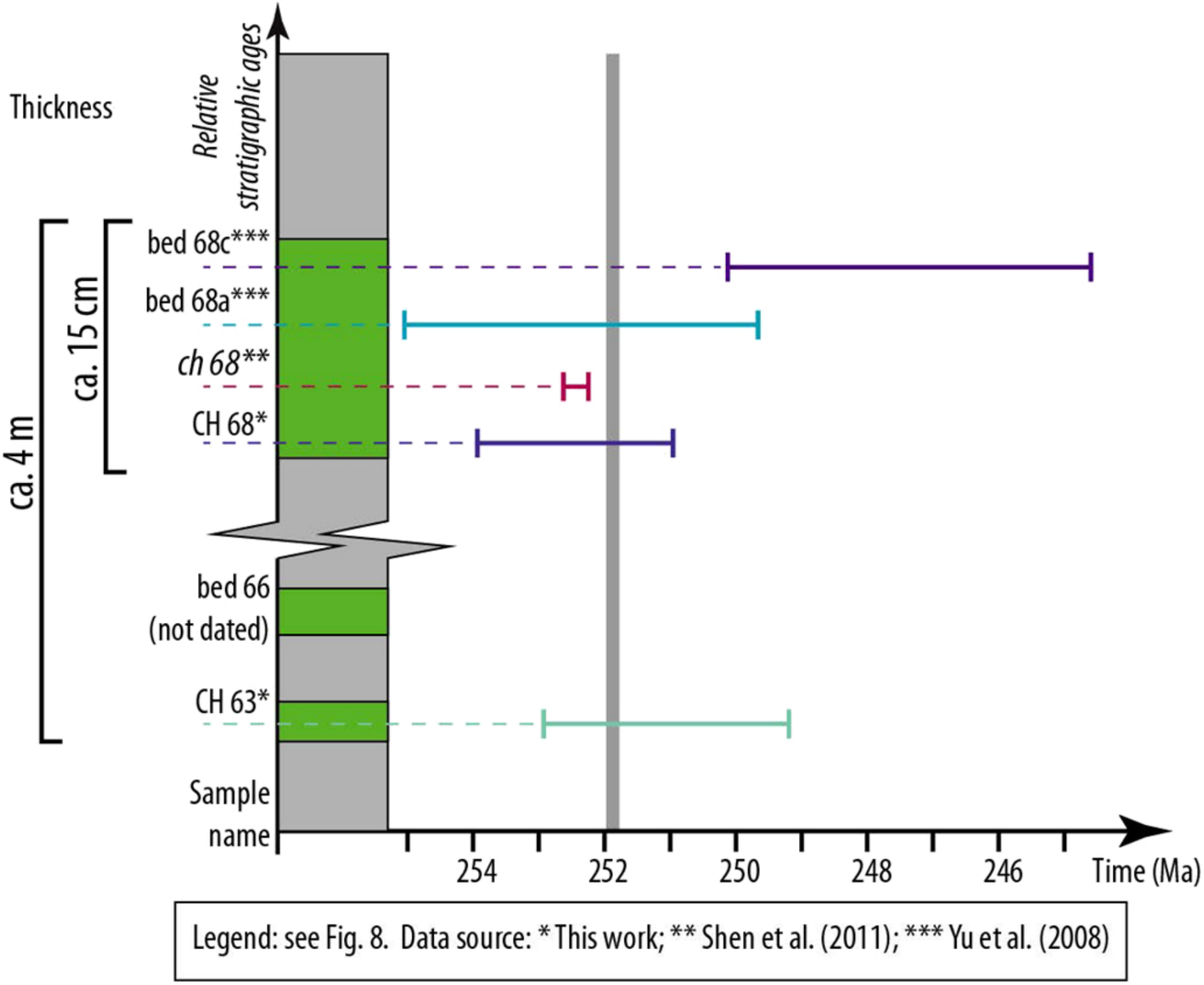

Thickness
Relative stratigraphic ages
ca. 4 m
ca. 15 cm
bed 68c***
bed 68a***
ch 68**
CH 68*
bed 66
(not dated)
CH 63*
Sample name
254
252
250
248
246
Time (Ma)
Legend: see Fig. 8. Data source: * This work; ** Shen et al. (2011); *** Yu et al. (2008)

Figure 9

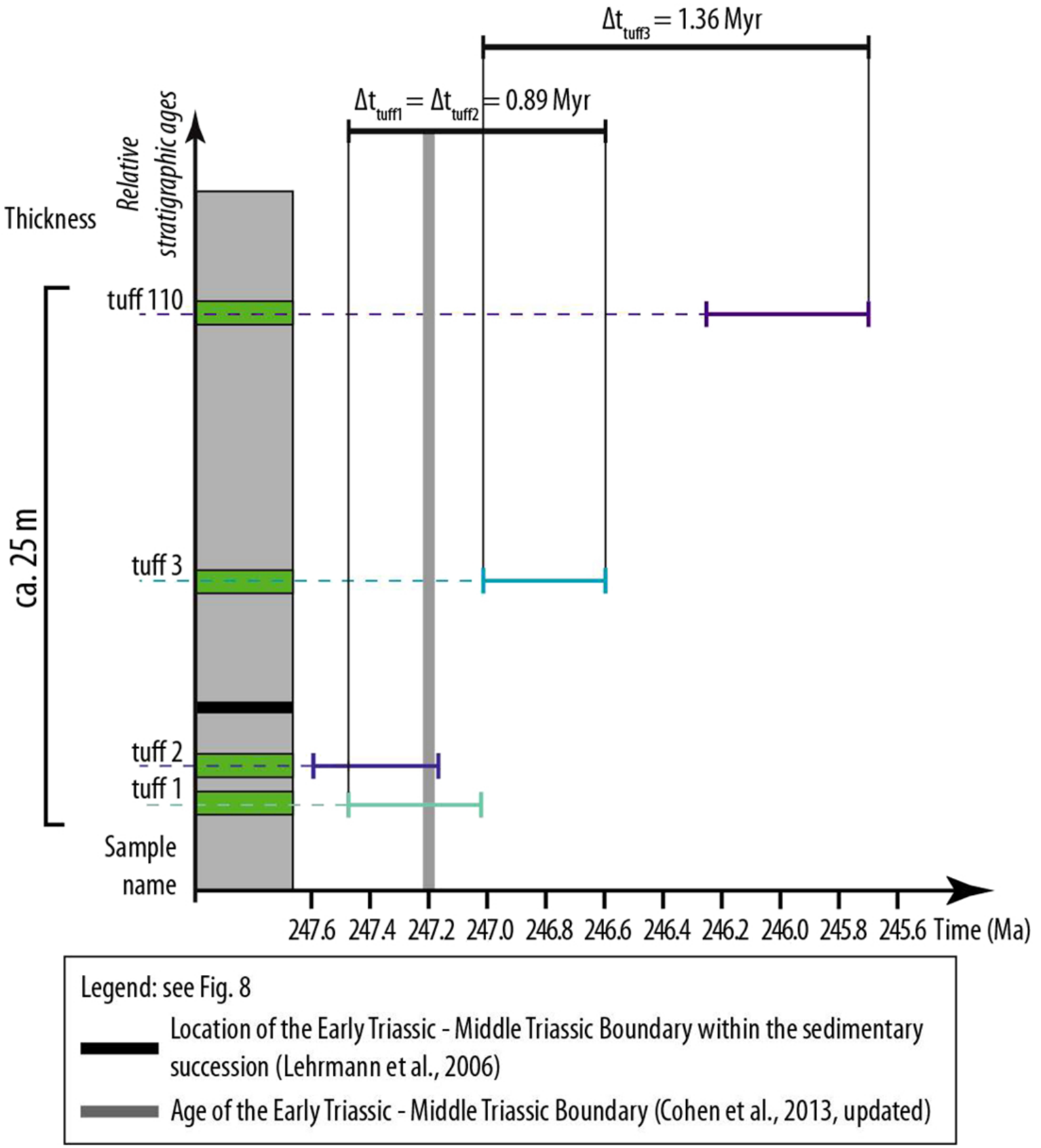

Δt tuff3 = 1.36 Myr
Δt tuff1 = Δt tuff2 = 0.89 Myr
Relative stratigraphic ages
Thickness
tuff 110
tuff 3
tuff 2
tuff 1
ca. 25 m
Sample name
247.6 247.4 247.2 247.0 246.8 246.6 246.4 246.2 246.0 245.8 245.6 Time (Ma)
Legend: see Fig. 8
Location of the Early Triassic - Middle Triassic Boundary within the sedimentary succession (Lehrmann et al., 2006)
Age of the Early Triassic - Middle Triassic Boundary (Cohen et al., 2013, updated)

Figure 10

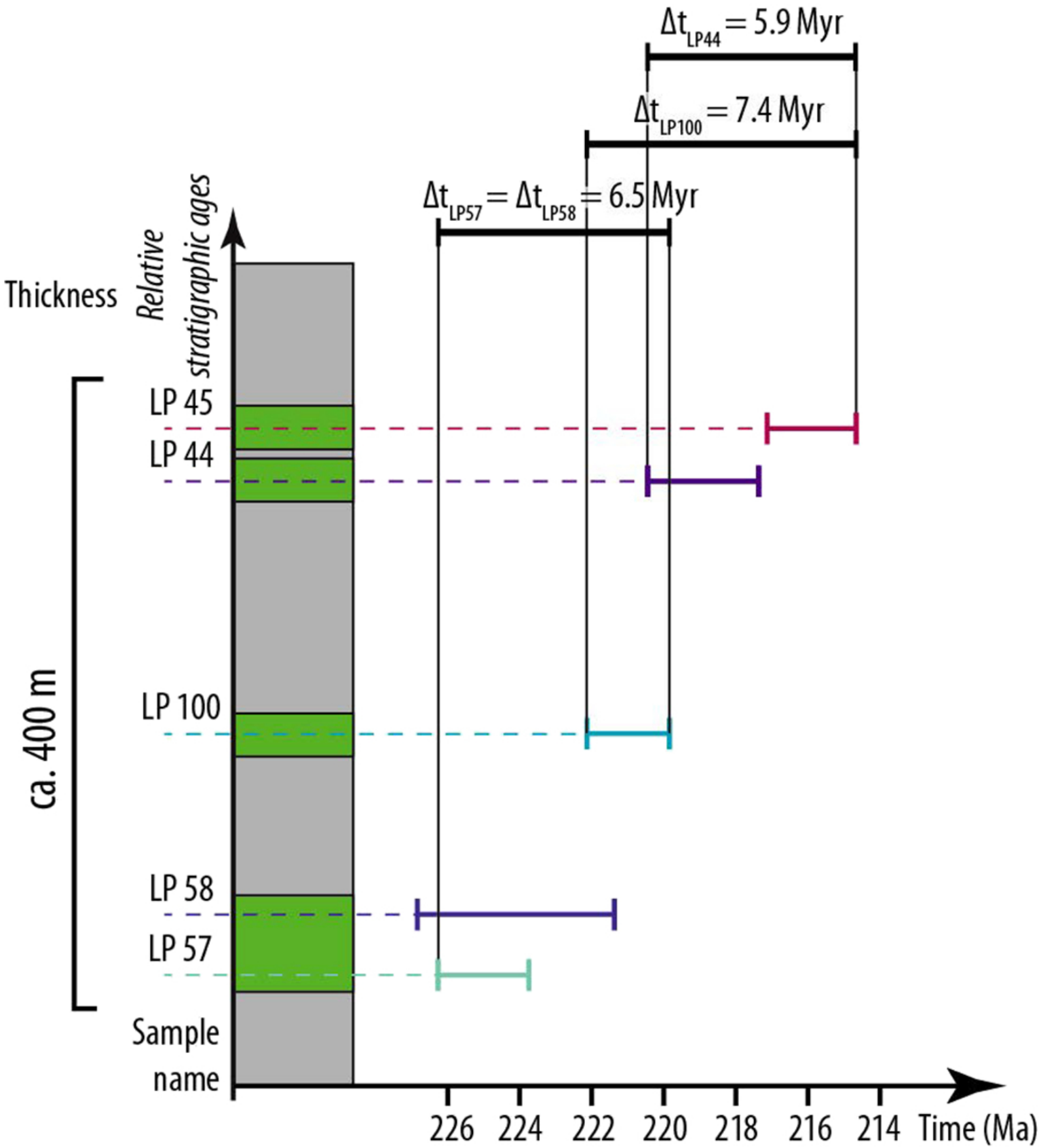

Δt LP44 = 5.9 Myr
Δt LP100 = 7.4 Myr
Δt LP57 = Δt LP58 = 6.5 Myr
Thickness
Relative stratigraphic ages
LP 45
LP 44
LP 100
LP 58
LP 57
ca. 400 m
Sample name
226
224
222
220
218
216
214
Time (Ma)

Figure 11

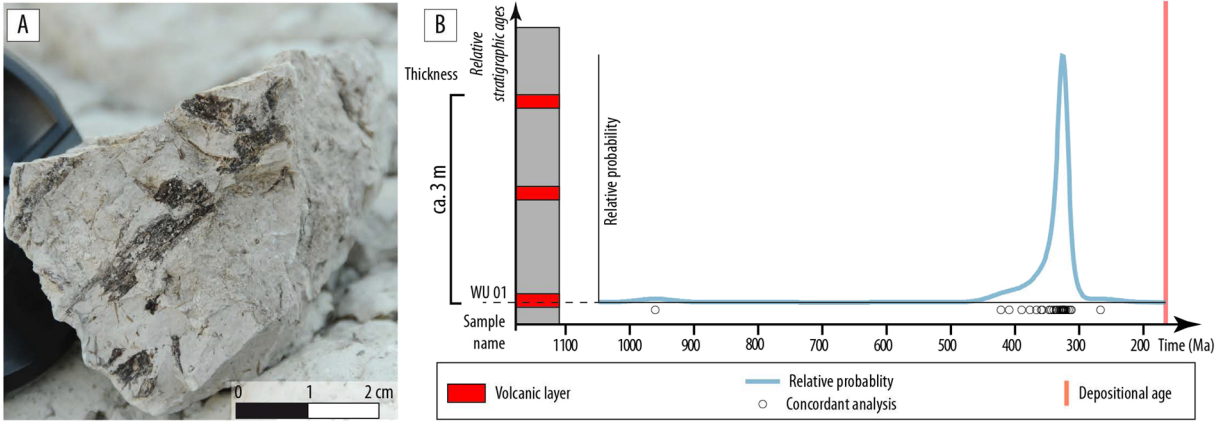

A
0
1
2 cm
B
Thickness
Relative stratigraphic ages
ca. 3 m
Relative probability
WU 01
Sample name
1100
1000
900
800
700
600
500
400
300
200
Time (Ma)
Volcanic layer
Relative probablity
Concordant analysis
Depositional age

Figure 12

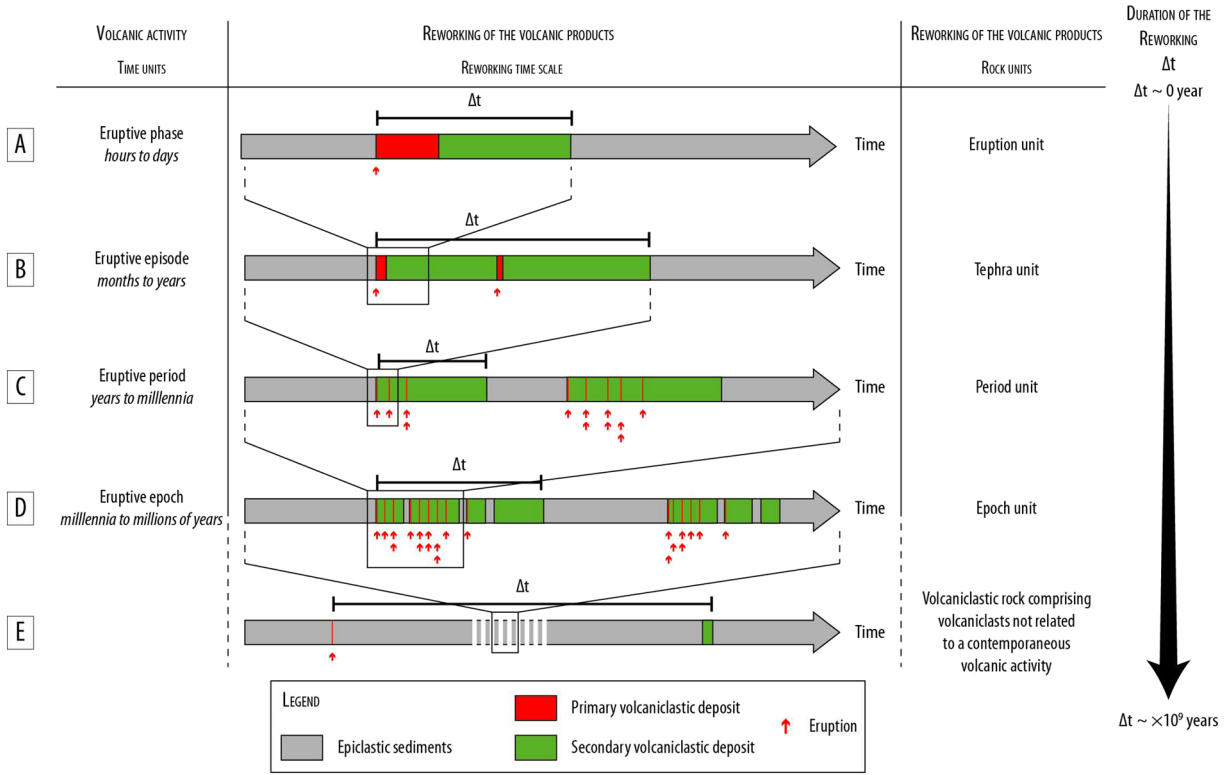

Volcanic activity
Time units
Reworking of the volcanic products
Reworking time scale
Reworking of the volcanic products
Rock units
Duration of the Reworking
Δt
Δt ~ 0 year
A
Eruptive phase
hours to days
Δt
Time
Eruption unit
B
Eruptive episode
months to years
Δt
Time
Tephra unit
C
Eruptive period
years to milllennia
Δt
Time
Period unit
D
Eruptive epoch
milllennia to millions of years
Δt
Time
Epoch unit
E
Δt
Time
Volcaniclastic rock comprising volcaniclasts not related to a contemporaneous volcanic activity
Δt ~ ×10⁹ years
Legend
Primary volcaniclastic deposit
Eruption
Epiclastic sediments
Secondary volcaniclastic deposit

Figure 13

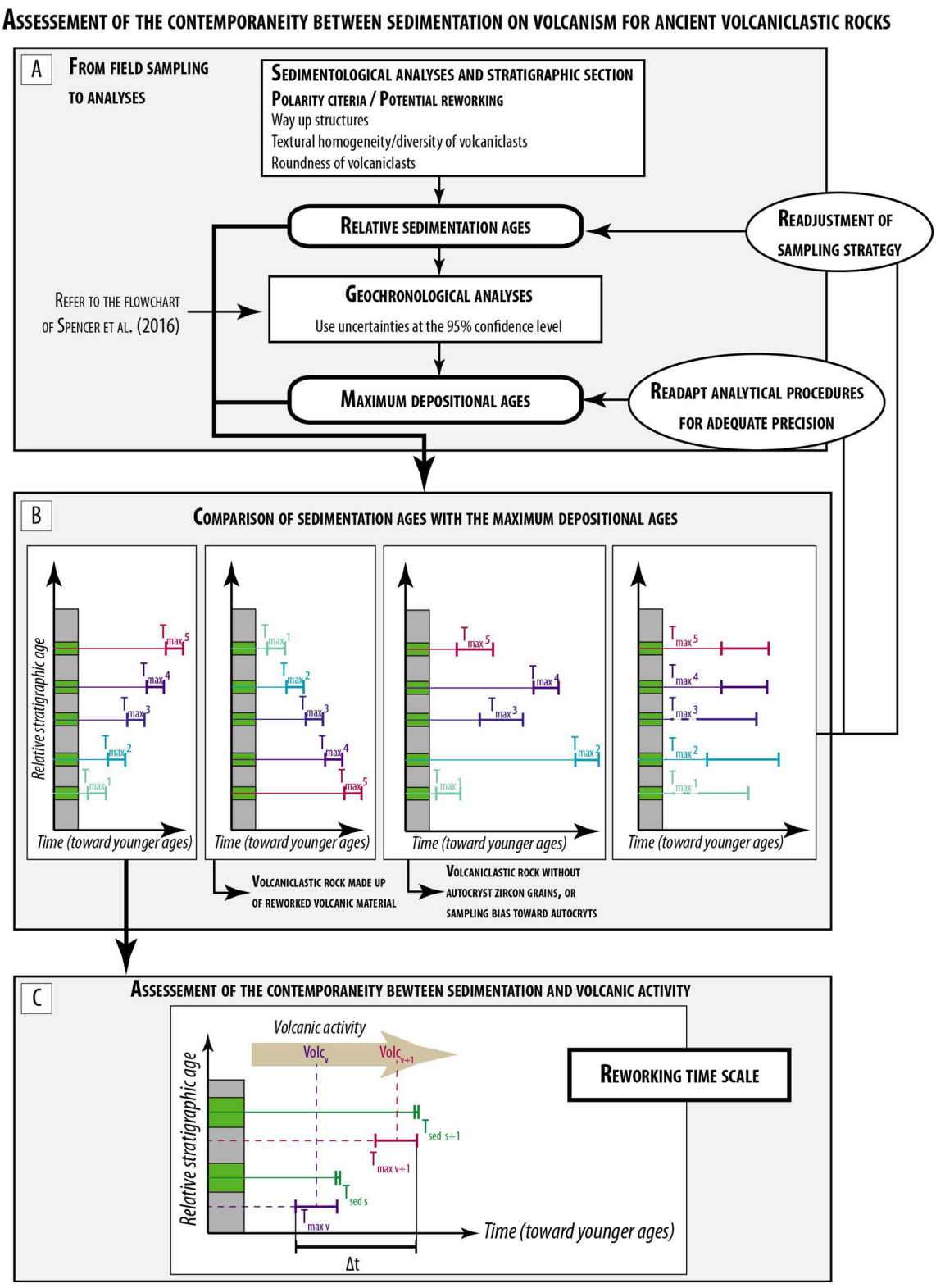

ASSESSEMENT OF THE CONTEMPORANEITY BETWEEN SEDIMENTATION ON VOLCANISM FOR ANCIENT VOLCANICLASTIC ROCKS
A
FROM FIELD SAMPLING TO ANALYSES
SEDIMENTOLOGICAL ANALYSES AND STRATIGRAPHIC SECTION
POLARITY CITERIA / POTENTIAL REWORKING
Way up structures
Textural homogeneity/diversity of volcaniclasts
Roundness of volcaniclasts
RELATIVE SEDIMENTATION AGES
READJUSTMENT OF SAMPLING STRATEGY
REFER TO THE FLOWCHART OF SPENCER ET AL. (2016)
GEOCHRONOLOGICAL ANALYSES
Use uncertainties at the 95% confidence level
MAXIMUM DEPOSITIONAL AGES
READAPT ANALYTICAL PROCEDURES FOR ADEQUATE PRECISION
B
COMPARISON OF SEDIMENTATION AGES WITH THE MAXIMUM DEPOSITIONAL AGES
Relative stratigraphic age
Time (toward younger ages)
VOLCANICLASTIC ROCK MADE UP OF REWORKED VOLCANIC MATERIAL
VOLCANICLASTIC ROCK WITHOUT AUTOCRYST ZIRCON GRAINS, OR SAMPLING BIAS TOWARD AUTOCRYTS
C
ASSESSEMENT OF THE CONTEMPORANEITY BEWTEEN SEDIMENTATION AND VOLCANIC ACTIVITY
Volcanic activity
REWORKING TIME SCALE
Δt

Figure 14